

## **Supplementary Information for** The Contributions of Rare Inherited and Polygenic Risk to ASD in Multiplex Families

Matilde Cirnigliaro<sup>#</sup>, Timothy S Chang<sup>#\*</sup>, Stephanie A Arteaga<sup>#</sup>, Laura Pérez-Cano, Elizabeth K Ruzzo, Aaron Gordon, Lucy K Bicks, Jae-Yoon Jung, Jennifer K Lowe, Dennis P Wall, Daniel H Geschwind<sup>\*</sup>

\*Daniel H Geschwind and Timothy S Chang  
Emails: dhg@mednet.ucla.edu; timothychang@mednet.ucla.edu

### **This PDF file includes:**

- Supplementary text
- Figures S1 to S11
- Tables S1 to S2
- Datasets S1 to S5
- SI References

## Supplementary Information Text

### Extended Technical Description of Results

#### *Multiplex Families*

Of the 1,004 multiplex ASD families, 714 families have 2 fully-phaseable autistic children (71.1%), 109 families have 3 fully-phaseable autistic children (10.8%), 8 families have 4 fully-phaseable autistic children (0.8%), 4 families have 5 fully-phaseable autistic children (0.4%), and 368 families have at least 1 fully-phaseable nonautistic child (36.7%). Among the fully-phaseable children, 1,620 are males and 634 are females. We also utilized 76 families with monozygotic concordant pairs to inform quality control (1). Dataset S1 provides information about the samples, including sex, ethnicity, phenotype, and familial relationship.

#### *Overall genetic architecture and transmission patterns in multiplex families*

Our WGS quality metrics were within expected range, including a transition to transversion ratio of 2.155, a heterozygous to non-reference homozygous ratio of 1.6, and dbSNP concordant rate of 99.92%. We retained high quality variants by using our WGS processing pipeline, which conducts filtering such as removing variant calls for samples with a genotype quality (GQ) < 25, depth (DP) < 10 and alternate allele depth to depth (ALT AD/DP) < 0.2 (SI Methods, Figure S2).

The mean number of rare inherited variants (MAF < 0.001, see SI Methods for additional quality criteria), private inherited variants, and rare de novo variants (protein truncating, missense or synonymous) per subject was 145.5, 32.4, and 0.46 respectively.

For private inherited variants we found no excess of protein-truncating variants (PTVs) (SI Methods, logistic regression,  $P = 0.79$ ) and missense variants (logistic regression, mis3  $P = 0.58$ ; MPC  $\geq 1$   $P = 0.46$ , MPC  $\geq 2$   $P = 0.81$ ) in autistic children (Figures S4G and S5C). The same held true when limiting the analysis to private inherited PTV and missense variants in highly constrained genes (logistic regression, pLI  $\geq 0.9$  mis3  $P = 0.48$ ; pLI  $\geq 0.9$  MPC  $\geq 1$   $P = 0.97$ ; pLI  $\geq 0.9$  PTV  $P = 0.20$ ; pLI  $\geq 0.995$  mis3  $P = 0.82$ ; pLI  $\geq 0.995$  MPC  $\geq 1$   $P = 0.39$ ; pLI  $\geq 0.995$  PTV  $P = 0.70$ ) (Figures S4H and S4I). We also defined constrained genes as those with LOEUF score < 0.35 and got variant burden comparison results consistent with those based on pLI (Figure S5F). Per gene LOEUF scores were downloaded from gnomAD v2.1.1 public repository.

We compared rare de novo variant rates between AGRE multiplex families and ASD simplex family-based collections to quantify differences in ASD genetic architecture (Figure S6, Dataset S5). Overall, we observed a significant strong depletion of rare de novo missense MPC  $\geq 1$  variants, missense MPC  $\geq 2$  variants, synonymous variants, and PTVs in (i) all genes, (ii) pLI  $\geq 0.9$  genes, and (iii) pLI  $\geq 0.995$  genes for autistic children in AGRE versus SSC (2) and in AGRE versus ASC+SSC (3) (Figure S6A-S6C). Results were more variable for the nonautistic children. In general, as expected, we found no rate differences between cohorts for most rare de novo variant sets. AGRE nonautistic children showed no differences in rate of rare de novo missense MPC  $\geq 2$  variants and PTVs in all genes compared to SSC and ASC+SSC nonautistic children (Figure S6A). AGRE nonautistic children showed a significant lower rate of rare de novo missense MPC  $\geq 1$  variants and synonymous variants in all genes compared to SSC nonautistic children (Figure S6A). For highly constrained genes (pLI  $\geq 0.9$  and pLI  $\geq 0.995$ ), we observed that even AGRE nonautistic children showed a significant depletion of rare de novo PTVs compared to SSC nonautistic children (Figure S6B-S6C). A similar signal was also found for missense MPC  $\geq 1$  variants and synonymous variants (Figure S6B-S6C).

### *Rare Inherited PTV Burden of Known ASD Risk Genes in Multiplex Families*

We compared rates of rare de novo and rare inherited PTVs in KARGs between AGRE multiplex families and ASD simplex family-based collections to quantify differences in ASD genetic architecture (Figure S9C, Dataset S5). AGRE autistic children showed a significant depletion of rare de novo PTVs in known ASD risk genes compared to SSC (2) (Poisson test,  $P = 2e^{-9}$ ,  $\log_2(\text{rate ratio}) = -2.26$ ) and to ASC+SSC (3) (Poisson test,  $P = 9e^{-7}$ ,  $\log_2(\text{rate ratio}) = -1.84$ ) autistic children, whereas variant rates were not different for nonautistic children (Figure S9C, Dataset S5). When comparing rates of rare inherited PTVs in KARGs for autistic children between AGRE and ASC+SSC (3), we found a significant enrichment signal for AGRE multiplex family-based cohort (Poisson test,  $P = 3e^{-19}$ ,  $\log_2(\text{rate ratio}) = -1.34$ ) (Figure S9C, Dataset S5).

Given the lower female to male ratio of ASD and multiple threshold theory of a female protective effect (4–6), we examined rare inherited PTVs in known ASD risk genes by sex. There was no difference in mean number of rare inherited PTVs in known ASD risk genes in autistic females versus autistic males (logistic regression,  $P = 0.94$ , Figure S9D, SI Methods), or autistic versus nonautistic children stratified by sex (Figure S9D). Both paternal and maternal inheritance of variants has been associated with ASD risk (7, 8). We observed no difference between the two modes of inheritance in this cohort (Figure S9E), although we acknowledge that larger population scale studies may be needed to see more subtle differences.

We also evaluated known risk genes for ASD and developmental delay (DD) (9), which totaled 208 genes (Dataset S3). Similar to observations in known ASD risk genes, the ASD and DD risk genes showed an increase in the number of inherited PTVs ( $p = 0.027$ , OR = 1.64, Figure S9A) in autistic children. There was no significant difference of known risk genes for ASD and developmental delay by sex (Figure S9D) or inheritance type (Figure S9E).

We found three families in which two autistic children inherited the same PTV pair in two different KARGs (Figure S10). Interestingly, in family A, of the three autistic dizygotic twins, the two females inherited PTVs in both *RANBP17* and *WDFY3* from the father, while the male did not. Intriguingly, the two female autistic twins had their first steps and phrases much later than their male autistic twin who, in contrast to them, did not show severely impaired social behavior and social interaction skills. In family B, the two autistic siblings inherit rare PTVs in both *CAPN12* and *FBXL13* from the father, while the nonautistic child has inherited only the *FBXL13* variant. In family C, both autistic children inherited a PTV in *MFRP* from the father and a PTV in *SHANK3* from the mother.

We tested for significance of oligogenic transmission of KARG rare inherited PTVs through two direct approaches. We tested the enrichment of autistic children with 2 rare inherited KARG PTVs among children with 1 rare inherited KARG PTV and found no significance (Fisher's exact test  $P = 1$ ). We also identified families where there were 2 or more KARG PTVs among parents (N families = 12), and tested the association of double hits in autistic children (6 out of 26 autistic children in 12 families) using a binomial test and found no significance (binomial test  $P = 1$ ). Therefore, we had no significant evidence supporting the oligogenic or two-hit inheritance model rare inherited KARG PTVs in the current cohort autistic children. Bigger sample sizes would be needed to investigate this interesting phenomenon (Figure S10).

### *ASD Polygenic Score is Overtransmitted in Autistic Children with Inherited Variants and Associated with Relevant Phenotypes*

The additive effect of ASD PGS to ASD rare inherited variation was not observed for PGS for schizophrenia (SCZ), bipolar disorder (BD), and educational attainment (EA) (Figure S11A, SI Methods).

We did not find overtransmission of PGS in children showing a delayed language

development when testing PGS for SCZ, BD, and EA (Figure S11B, SI Methods).

We did not observe any difference in the contribution of common variation to social behavior among children with severe or mild social impairment when testing PGS for SCZ, BD, and EA (Figure S11C, SI Methods).

## Methods

### ASD multiplex family samples

The Rutgers University Cell and DNA Repository (RUCDR; Piscataway, NJ) provided our purified DNA. Whenever possible, whole blood DNA was used; for many samples, however, only lymphoblastoid cell line (LCL) DNA was extracted at the time of recruitment.

There is an overlap of 431 samples, including 235 probands, between the AGRE multiplex families from this study and the recent MSSNG study (10). This information has been included in Datasets S1 and S4 to facilitate future mega-analyses.

If not otherwise specified, our analyses included a subset of 2,254 children (1,836 autistic and 418 nonautistic) whose parents had both undergone sequencing and passed QC.

### Control cohorts

We refer to several control cohorts throughout the manuscript that we have used to assess variant frequencies in non-ASD samples. These cohorts are described below.

#### *Publicly available databases*

Annotations from publicly available databases were obtained from ANNOVAR and include: the 1000 genomes project (1000g2015aug\_all) (11), gnomAD (version 2.0.2) (12), the Exome Aggregation Consortium (exac03nonpsych) (13), the NHLBI Exome Sequencing Project (esp6500siv2\_all) (<http://evs.gs.washington.edu/EVS/>), and allele frequency estimates from whole-genome sequenced unrelated, healthy subjects (<http://www.completegenomics.com/public-data/69-genomes/>, cg46).

#### *UCLA internal controls*

The “UCLA internal controls” referred to throughout this manuscript are comprised of 379 unrelated, whole-genome sequenced samples with *Progressive Supranuclear Palsy* (PSP). ASD and PSP have no known etiological overlap or comorbidity.

#### *Healthy Non-Phaseable (HNP) samples*

These samples likely harbor genetic variants associated with ASD, and so provide allele frequency estimates that are generally more permissive when filtering for inherited risk variants.

### Whole-genome sequencing and data processing

Whole-genome sequencing was conducted on DNA samples through New York Genome Center (NYGC). Following DNA sample quality and quantity assessment, genotyping was performed using Illumina Infinium Human Exome-12 v1.2 or Infinium Human Core Exome microarrays (San

Diego, CA). The genome-wide genotyping data was subsequently used to confirm sample identity and conduct sex checks in PLINK v1.07 (14). VerifyIDintensity (VII) (15) was used to assess contamination; samples with two or more modes of contamination greater than 3% were excluded from sequencing. Samples that passed identity and quality checks were then sequenced at NYGC using the Illumina TruSeq Nano library kits and Illumina's HiSeq X (San Diego, CA) (1).

WGS data were processed through the same bioinformatics pipeline, adapted from GATK's best practices (16, 17). The bioinformatics processing steps are outlined in our previous study manuscript (1), with the only difference being that GATK tools were updated to version 3.4 and Picard MarkDuplicates tool to version 1.83.

### **Quality control assessment**

WGS data underwent standard quality control checks to ensure the accuracy of sequencing and variants, as well as sample identity. Checks were conducted on samples for relatedness, duplicates, contamination, sequencing coverage, variant quality (using GATK's VariantEval module), concordance between genotyping chip and WGS data, and concordance between self-declared sex and observed biological sex. A total of 4,551 individuals from 1,004 ASD families, from the Autism Genetic Resource Exchange (AGRE) passed quality control (Dataset S1).

#### *Whole-genome sequence coverage*

We calculated genome-wide per-base sequencing coverage for each sample using SAMtools v1.2 (18). Custom scripts were used to calculate (i) average coverage and (ii) percentage of the genome (excluding gap regions, downloaded from the UCSC table browser) covered at 1X, 10X, 20X, 30X, and 40X. On average across all samples, 99.2% of bases were covered at a depth of  $\geq 10X$  (Figure S1A-E).

### **Variant inheritance classifications**

Variants were classified into one of eight inheritance types: (i) de novo, (ii) paternally inherited, (iii) maternally inherited, (iv) missing, (v) uncertain, (vi) unknown phase, (vii) newly homozygous, or (viii) newly hemizygous. Definitions for newly homozygous, newly hemizygous, unknown phase, and uncertain inheritance types are available in our previous manuscript describing the analysis of a subset of this cohort (1). All VQSR failed and multi-allelic variants were excluded before reaching this classification step. Variants were also required to have a read depth of  $\geq 10X$ , genotype quality of  $\geq 25$ , and alternative allele reads/total reads ratio of  $\geq 0.2$ .

### **Defining rare inherited and private variants**

Rare inherited variants were defined as SNVs and indels with an allele frequency (AF)  $\leq 0.1\%$  in publicly available databases (1000g2015aug\_all, ExACv3.0, cg46, gnomAD), internal controls, and HNPs (SI Appendix describing control cohorts). These variants were also restricted to those not flagged as low-confidence in the Genome in a Bottle Consortium (GIAB) (19) and missing in  $\leq 25\%$  of controls.

Private variants were defined as SNVs and indels observed in only one cohort family (AF  $\sim 0.05\%$ ) and missing in  $\leq 25\%$  of HNPs. In addition, private variants were required to meet the following criteria: (i) not observed among control cohorts (AF = 0), (ii) missing in  $\leq 25\%$  of PSP controls, (iii) not flagged as low-confidence in the GIAB Consortium. We only analyzed private variants in the 2,254 fully-phaseable children in our study.

## Noncoding analyses

### *Definition of noncoding variants*

Noncoding variants include SNVs and indels labeled with one of the following VEP consequences: “3\_prime\_UTR\_variant”, “5\_prime\_UTR\_variant”, “downstream\_gene\_variant”, “upstream\_gene\_variant”, “feature\_elongation”, “feature\_truncation”, “intergenic\_variant”, “intron\_variant”, “mature\_miRNA\_variant”, “non\_coding\_transcript\_exon\_variant”, “non\_coding\_transcript\_variant”, “regulatory\_region\_ablation”, “regulatory\_region\_amplification”, “regulatory\_region\_variant”, “TF\_binding\_site\_variant”, “TFBS\_ablation”, “TFBS\_amplification” (1). To ensure strict filtering of noncoding variants, only the first most damaging consequence associated with a single variant was taken into account if there were multiple annotations available. We only considered noncoding variants that had not been flagged as low-confidence by the GIAB consortium.

### *Description of noncoding variant sets tested*

The noncoding rare inherited, private inherited, and rare de novo variant sets were further refined before quantitative burden testing. The first refined sets of noncoding variants used (Figure S7A-C) consist of those mapping to promoters, defined as 2kb or 10kb upstream, and 1kb downstream (3kb and 11kb promoters, respectively) from the TSS, by referencing the longest transcript for each gene (for transcripts of identical length, the lower Ensembl Transcript ID was used). Rare inherited and private inherited variants mapping to 3kb promoters were further filtered (Figure S7D-E) by keeping those in promoters of genes belonging to ASD risk gene sets identified and defined in this study, the 74 TADA genes (with FDR < 0.1 in TADA-mega analysis), and the 152 known ASD risk genes. We also specifically focused on variants mapping to TFBSs located within 11kb promoters (Figure S7F-H). As single global maps of genomic regions bound by TFs to use for variant filtering we chose (1) cis-regulatory modules (CRMs) from the whole UniBind database (20), and highly reliable (category A) (2) cistromes and (3) cismotifs, as defined in (21). Finally, we took advantage of a new colocalization approach for interpreting the functionality of noncoding regions (22), which evaluates both their sequence constraint within the human lineage and their tissue- or cell type-specific regulatory role, by keeping variants in both 11kb promoters and across the whole genome that map to the 10-tissue catalogue of brain-specific colocalized regions (<http://www.funlda.com/colocalization/region>) (Figure S7I-K).

### *Samples included for noncoding analyses*

Noncoding rare and private inherited analyses included variants from 2,254 fully-phaseable children ( $N_{\text{aut}} = 1,836$ ,  $N_{\text{nonaut}} = 418$ ). Noncoding RDNVs were restricted to 1,443 non-ARC outlier samples ( $N_{\text{aut}} = 1,164$ ,  $N_{\text{nonaut}} = 279$ ) and variants identified as high-confidence by ARC.

### *Noncoding variant quantitative burden testing*

Noncoding variants belonging to each refined set were counted for each child and used to perform regression, together with child phenotypic group, sex, and sample source of DNA. First, we modeled the response variable “variant count per child” by including the predictor variables “child phenotype”, “child sex”, and “sample source of DNA” through Poisson / quasi-Poisson / negative binomial regression models (R stats glm() function and MASS glm.nb() function were used). The negative binomial models were the best model to correct for overdispersion of the count data. For rare de novo variants and both rare inherited and private inherited variants mapping to 3kb promoters of genes belonging to ASD risk gene sets (Figure S7D-S7E), we checked for potential zero-inflation of the count data and additionally built zero-inflated Poisson and zero-inflated negative binomial regression models (R pscl zeroinfl() function was used). Even

for these variant sets, the negative binomial models were the best to predict zero counts. Alternatively, we modeled the response variable “child phenotype” by including the predictor variables “variant count per child”, “child sex”, and “sample source of DNA” through logistic regression. For all models built, we used (1) the residual deviance to perform a goodness of fit test for the overall model and (2) the difference between the residual deviance for the model with predictors and for the null model to test the significance of the overall model. These tests confirmed that the logistic regression models were the only models with a good fit and significance for the overall model. For this reason, although all approaches for quantitative burden testing described above returned consistent results, in this paper we chose to report those from logistic regression analyses (see equation in *Comparison of rates of variants in autistic and nonautistic children* section from SI Methods) (Table S1) for which we also computed power (Table S2). ASD odds ratio (OR) values were obtained by exponentiating the estimated regression coefficients. P-values < 0.05 were considered significant.

#### *Power analysis for quantitative burden testing through logistic regression*

Power for quantitative burden testing through logistic regression was computed for each tested variant set by simulation.

We used a post-hoc approach, computing power for the observed ASD ORs and at the current sample sizes for all three predictor variables “variant count per child”, “child sex”, and “sample source of DNA” (Table S1). We adopted three different simulation strategies to generate simulated data to use as new input to rerun logistic regression and estimate power, based on (1) the R `simr powerSim()` function (23) and on two custom functions named (2) “sample” and (3) “random”, respectively. The first two strategies use bootstrapping, which resamples from the existing dataset, while the “random” strategy uses random variable generation and regression coefficients from the logistic model for the three predictor variables to compute the simulated response variable “child phenotype”. Quality of simulations was assessed by visualizing both simulated variables and resulting logistic regression coefficients. The three simulation strategies returned very consistent results (Table S2): in this paper we chose to report those obtained with the “sample” custom function strategy (Table S2 and Figures S7L-S7N).

Power was estimated as the proportion of significant regression results ( $p < 0.05$ ) over 1,000 simulations, together with 95% confidence intervals for this value (Table S2). In addition, for each tested variant set, we built a power curve specific to the variant count per child predictor, for the observed ASD OR, and at specific increasing sample sizes (inherited: 2,000-9,000; rare de novo: 1,000-8,000). Curves were fitted by local regression for visualization. We used strategies 2 and 3 to build these power curves and obtained reproducible results.

The post-hoc power analysis confirmed that the observed ASD ORs for the noncoding variant sets tested are too small to be detected at the current sample sizes, consistent with results from previous analysis of ASD simplex families (24) (Table S2). The power curves built for increasing sample sizes showed that a sample size of at least 8,000 fully-phaseable children would give sufficient power to detect the observed ASD OR for private inherited variants mapping to 11kb promoter regions (at least 9,000 fully-phaseable children for the following private inherited sets: 3kb promoters, cistromes, cismotifs, and brain colocalized regions across the whole genome), whereas a sample size of at least 7,000 fully-phaseable children would allow the detection of the observed ASD OR for rare de novo variants mapping to brain colocalized regions across the whole genome (Figures S7M-S7N and Table S2 (as reference for ASD ORs and p-values for each set)). Notably, the increasing sample sizes tested would not give sufficient power to detect the observed ASD OR for any of the sets of rare inherited variants (Figure S7L and Table S2).

## Artifact Removal by Classifier (ARC)

The Artifact Removal by Classifier (ARC) supervised model was designed to separate true rare de novo variants from LCL-specific genetic aberrations or other kinds of artifacts, such as sequencing and mapping errors (<https://github.com/walllab/iHART-ARC>). Details on the training, features, and performance evaluation of ARC are provided in our previous manuscript (1).

### *ARC outlier samples*

When applied to all 2,254 children (partially or fully-phaseable), we found a subset of outlier samples (fully-phaseable  $n = 657$ ) that had an ARC score less than 0.4 for >90% of their raw de novo variant calls. We excluded all ARC outlier samples from downstream analyses that involved de novo variants unless otherwise mentioned.

## De novo variant rate versus paternal age

We analyzed the correlation between paternal age and de novo variant rate in 1,157 fully-phaseable, autistic children (excluding MZ twins, ARC outliers, and 7 samples without paternal age information). Details on the linear model used in this analysis are available in our previous study (1). We observed a significant signal after running ARC ( $P < 2.2e^{-16}$ ), but not prior to application of ARC (Figure S3D). According to our study, the RDNV rate increased by 1.02 per year of paternal age (95% CI = 1.02-1.03), consistent with previously published studies (9, 25–27).

Paternal age was not a significant predictor variable of the logistic regression models used for quantitative burden testing of the rare de novo coding sets, and since it was missing for 7 autistic children, we preferred not to incorporate it as covariate and include all 1,164 autistic children in these analyses.

## Rates for rare de novo variants

We only considered de novo variants in the 2,254 fully-phaseable children for analysis. Rare de novo variants were defined as: (i) absent in all controls, (ii) given an ARC score  $\geq 0.4$ , (iii) missing in less than or equal to 25% of controls, (iv) not flagged as low-confidence by the GIAB consortium, (v) not present in an ARC outlier sample ( $n = 657$ ). Due to the use of LCL MZ twins ( $n = 154$ ) as the ARC training set, all MZ twin de novo variants were excluded from de novo rate calculations. Consequently, all de novo variant rate calculations were performed using 1,443 fully-phaseable non-MZ twins and non-ARC outliers ( $N_{\text{aut}} = 1,164$ ;  $N_{\text{nonaut}} = 279$ ).

Our results suggest a mean genome-wide rate of 52.8 RDNVs per child (Figure S3B), which is consistent with previously reported rates (mean = 64.4; range 54.8-81) (28–30, 27, 31, 32). We used the Wilcoxon rank sum test to determine if the number of de novo variants was significantly different in autistic versus nonautistic children.

## Comparison of rates of variants in autistic and nonautistic children

For rare inherited, rare de novo, and private inherited variants, we compared the rates (number of variants per child) for missense, synonymous, and protein-truncating variants in autistic versus nonautistic children. We used the logistic regression model:

$$\log \left[ \frac{P(\text{Phenotype} = \text{Autistic})}{1 - P(\text{Phenotype} = \text{Autistic})} \right] = \alpha + \beta_1(\text{Variants\_per\_child}) + \beta_2(\text{Sex}) + \beta_3(\text{DNA\_source})$$

We performed this analysis with all genes and those with  $pLI \geq 0.9$  and 0.995 as well as  $LOEUF < 0.35$ .



## **TADA mega-analysis**

### *Samples and qualifying variants*

The sample sizes for the TADA-mega analysis are provided in Dataset S2. We note that 119 of the 424 AGRE samples included as “cases” in the original TADA analysis (33) with only transmitted PTVs accounted for, were able to have their DN PTV and mis3 variants accounted for in this AGRE multiplex family cohort. This was possible thanks to the sequencing of these samples (or their corresponding monozygotic twin) and their biological parents in this WGS study. The acquisition of these AGRE samples and the method used to count their DN PTV/mis3 variants and transmitted PTVs are outlined in our previous manuscript (1).

To enable future meta-analyses, we show in Dataset S4 the 431 samples in our study that overlap with MSSNG.

We annotated the DN mis3 variants in the cohort using the “probably damaging” PolyPhen-2 (34) v2.2.2r395 HumDiv predictions from the Whole Human Exome Sequence Space (WHES dataset). In cases where multiple qualifying variants in a gene were found in a sample, only the most damaging variant was retained.

DN PTV/mis3 variants counts are identified in 5,275 ASD individuals from AGRE multiplex families, SSC (35), and ASC (33), while counts for the transmitted and nontransmitted PTVs are compiled from 4,563 autistic individuals and 8,359 nonautistic controls collected from the ASC (33) and the selected AGRE multiplex families (Dataset S2). In addition, we calculated the counts of DN SmallDel in 4,687 ASD individuals from the SSC (36) and the AGP (37) (Dataset S2).

### *TADA parameters and analysis*

The TADA parameters used in this study match those used in our previous TADA mega-analysis (1). After performing the Benjamini-Hochberg correction on the TADA results, q-values (False Discovery Rate (FDR)) < 0.1 were considered significantly associated with ASD.

### *TADA simulations*

This approach was previously chosen and amply described for risk gene discovery on a subset of these AGRE multiplex families (1).

Briefly, we estimated the null TADA statistic for multiplex families by simulating Mendelian transmission and de novo mutation while keeping the observed TADA-qualifying variant counts per family and the family structures from the TADA mega-analysis unchanged.

The rare de novo protein-truncating and mis3 variants in each sample were randomly shuffled across all the genome genes by redrawing in proportion to the gene-specific mutation rates.

The occurrence of rare inherited PTVs in each sample was simulated by first randomly shuffling them across all genes in the corresponding parents and then, by randomizing Mendelian inheritance across all children, autistic and nonautistic, in the corresponding family (with 50% probability of transmission to each child in each simulation).

Small de novo deletions spanning N (2-7) genes in each sample were randomly shuffled across all contiguous N-gene sets by redrawing in proportion to the multi-gene mutation rates.

After getting the simulated variant counts for each dataset in the mega-analysis with 100,000 simulations, we ran TADA with the same parameters used in the original TADA mega-analysis. For each simulation, we got a combined Bayes factor (BF) per gene by multiplying those for each TADA-qualifying variant class. Finally, we used the distribution of combined BFs per gene across the 100,000 simulations (the distribution of the null TADA statistic) to derive a single simulation p-value per gene, reflecting how likely it is for each gene to observe a BF at least as extreme as the BF from the original TADA mega-analysis by chance (assuming no link between mutation rate, transmission rate, and autism). We computed simulation FDRs from p-values for the 18,472 genes included in the TADA analysis and considered genes with simulation FDR < 0.05 to be significantly associated with ASD.

### **Genes with large inherited PTV contribution**

Taking into account the rare inherited variant signal in our data, we aimed to identify TADA genes for which inherited PTVs account for a large portion of the qualifying variants. We adjusted the number of TADA-qualifying variants to include only variants where inheritance is known, ignoring PTVs from TADA mega-analysis ASC and SSC samples for which inheritance is unknown. We defined the total number of qualifying variants (N) in each TADA gene as  $N_{DN.PTV} + N_{DN.SmallDel} + N_{DN.Mis3} + N_{Inherited.PTV}$ . We identified genes that have a major contribution from inherited PTVs through two methods: (1) the inherited component of a gene ( $N_{Inherited.PTV}/N$ )  $\times 100\% \geq 70\%$ ; (2) the TADA association signal was strongly driven by inherited PTVs, meaning the Bayes Factor from inherited PTVs was greater than all other de novo variant classes ( $BF_{inheritedPTV} > BF_{dnPTV}$  &  $BF_{inheritedPTV} > BF_{dnSmallDel}$  &  $BF_{inheritedPTV} > BF_{dnMis3}$ ).

### **Fetal Single Cell Expression of TADA genes**

The mean expression and percent expressed were calculated within each cell type and hierarchically clustered using base stats R function `hclust()` with “complete” method on the scaled values of the mean normalized expression within a cell type. To find cell type-specific genes, the TADA genes were intersected with cell type enriched genes from (38). Enriched genes from (58) were found as follows: (i) Wilcoxon rank sum test using `FindAllMarkers` from Seurat R package (39), (ii) Bonferroni corrected  $p < 0.05$ , (iii) greater than a 0.2 log fold change of expression in a given cluster compared to all other clusters, and (iv) detected in >10% of cells in a cell type cluster. Expression Weighted Cell Type Enrichment (EWCE) (40) was performed to determine if TADA genes were enriched in cell types from (38) using 10,000 bootstrap simulations and a background set of all coding genes measured in (38).

### **Developmental Trajectory Analyses**

Briefly, hCS samples included six human induced pluripotent stem cell (hiPSC) lines derived from five different individuals that were cultured for up to 694 days in vitro. In total, 62 samples were collected for RNA sequencing (from four individuals, five hiPSC lines) at 13 timepoints. RNAseq libraries were prepared using Truseq stranded RNA RiboZero Gold (Illumina) and were sequenced using 100-bp paired end reads on an Illumina HiSeq 4000. Reads were then mapped to hg38 with Gencode v.25 annotations using STAR (v.2.5.2b) (41). Gene expression levels were quantified using RSEM (v.1.3.0) (42). Genes with low levels of expression (less than ten reads in more than 20% of the samples) were removed from the analysis. Outliers were then removed using standardized sample network connectivity (Z scores smaller than -3) (43). To quantify the technical variation in the RNA sequencing, we calculated the first five PCs of the Picard sequencing metrics (<http://broadinstitute.github.io/picard/>; v.2.5.0). These PCs, referred to as seqPC1–seqPC5, were then included in the linear model.

To help control for variability between the individuals racial background, we used the GATK (v.3.3) HaplotypeCaller to call single nucleotide polymorphism (SNPs) from the aligned reads (44). We filtered for sites with missing genotypes (>5%), rare minor allele frequency (<0.05) and out of Hardy–Weinberg equilibrium (<1e<sup>-6</sup>) (14). Genetic ancestry was inferred by running multidimensional scaling (MDS) on these high-quality SNPs together with HapMap3.3 (hg38). The first two MDS values, referred to as ancestryPC1/2, were then included in our linear model.

For principal component analysis (PCA), as well as to visualize single gene trajectories, gene expression was normalized using CQN (without quantile normalization, sqn = FALSE) (v.1.28.0) and ancestryPC1-2 and SeqPC1-5 were regressed out before batch correction using Combat (45) from the sva package (v.3.30.0) in R. Single gene trajectories' trend lines were fitted using the loess method (46) from the ggplot2 package (47) in R.

To quantify gene expression at each developmental stage in the BrainSpan RNA sequencing data (48), the cortical samples were aligned to hg38 using Gencode v.25 annotations via STAR (41). Gene expression was then quantified using the union exon model in featureCounts (49). We removed low quality samples in which the RNA integrity number (RIN) was lower than 8, or having less than 25% coding bases, or with ribosomal bases comprising more than 25% of total bases (as called by Picard tools). Genes with low levels of expression (less than ten mapped reads in more than 80% of the samples) in a given developmental stage were removed. We retained 196 samples from 24 individuals (9 female and 15 male).

We clustered the scaled normalized expression of hCS genes using hierarchical clustering on the Euclidean distance between genes. Cluster eigengenes were calculated using the module Eigengenes function from the WGCNA package (50). The gene in each cluster were correlated to the cluster module eigengene and the top five genes were annotated on the heatmap. The average expression per time point was calculated and trajectories' trend lines were fitted using the loess method (46) from the ggplot2 package (47). GO terms enrichment was performed using the enrichGO function from the clusterProfiler package (51) (v.3.12.0). Enrichment was performed on biological process and molecular function GO terms. All genes expressed in the hCS were used as background.

### **Known ASD Risk Genes (KARGs) Analysis**

A comprehensive list of 152 known ASD risk genes (KARGs) was generated by merging unique genes, with HGNC-approved gene names, identified at FDR < 0.1 in the current mega-analysis and previous TADA mega-analyses (1, 36, 52). The same rare qualifying variant classes as TADA were considered (Methods). Transmitted PTVs in ASD risk genes were identified in the 2,254 fully-phaseable children ( $N_{\text{aut}} = 1,836$ ,  $N_{\text{nonaut}} = 418$ ), while DN PTV or mis3 qualifying variants in ASD risk genes were restricted to those identified in the 1,443 non-ARC outlier samples ( $N_{\text{aut}} = 1,164$ ,  $N_{\text{nonaut}} = 279$ ).

The list of risk genes for ASD and developmental disorders (DDD) was generated by merging unique genes, with HGNC-approved gene names, from known ASD risk genes and the Deciphering Developmental Disorders study (9) with an FDR < 0.1. This gene set totaled 208 genes (Dataset S3).

### **Variant rate comparison between AGRE multiplex families and ASD simplex family-based collections**

#### *Available variant data from ASD simplex family-based collections*

We compared rates of coding variant sets from AGRE to those of curated sets from SSC (2) and ASC+SSC (3) to quantify the depletion of de novo variation and the enrichment for rare inherited variation observed in multiplex families. Annotated de novo coding variants identified in the SSC

were obtained from Zhou, *et al.* (2). This SSC dataset includes variants from 2,654 autistic children and 2,176 nonautistic children. Variants from this dataset were identified, filtered, and annotated similarly to those from AGRE (2). Aggregated per-gene counts for de novo and rare inherited variants identified in ASC+SSC participants were retrieved from Fu, *et al.* (3). This ASC+SSC dataset includes variants from 8,028 (5,606+2,422) autistic children and 2,460 (610+1,850) nonautistic children. Identification, filtering, and annotation of variants from this dataset (3) were performed differently from AGRE. In addition, the ASC samples include a small number of multiplex families' samples, mainly from AGRE (52). These two caveats make the comparison between AGRE and ASC+SSC (3) less ideal. We decided to still include this dataset in the analysis given its relevant large sample size ( $n = 10,488$ ). Despite these caveats, comparisons between AGRE and SSC and between AGRE and ASC+SSC gave very consistent results. As expected, based on the inclusion of some AGRE multiplex families in ASC, the observed depletion in rare de novo variation was always stronger when AGRE was compared to SSC only than to ASC+SSC. All available corresponding variant sets between cohorts were included in the analysis.

### *De novo coding variants*

We compared rates of de novo missense variants ( $MPC \geq 1$  and  $MPC \geq 2$ ), synonymous variants, and PTVs in (i) all genes, (ii)  $pLI \geq 0.9$  genes, and (iii)  $pLI \geq 0.995$  genes in AGRE versus SSC and in AGRE versus ASC+SSC. We performed these analyses separately for autistic and nonautistic children. AGRE autistic children included in the de novo variant analyses were 1,164, whereas AGRE nonautistic children were 279. In each cohort, for each variant set to test, we obtained counts in autistic and nonautistic children. Then, variant rates were compared by a Poisson test.  $p$ -values  $< 0.05$  were considered significant.

### *De novo and rare inherited PTVs in known ASD risk genes (KARGs)*

We compared rates of de novo PTVs in KARGs in AGRE versus SSC and in AGRE versus ASC+SSC for both autistic and nonautistic children. The available ASC+SSC dataset (3) reported the number of transmitted PTVs to autistic offspring; therefore, we compared rates of rare inherited PTVs in KARGs for autistic children in AGRE versus ASC+SSC. AGRE autistic children included in the rare inherited variant analyses were 1,836. The ASC+SSC dataset included variant counts for just 149 out of 152 KARGs. Testing was performed as described above.

## **Polygenic Transmission Disequilibrium Test (pTDT) Analysis**

### *Polygenic Scoring*

For ASD we used the ASD iPSYCH GWAS (this cohort overlaps with the PGC (Psychiatric Genomics Consortium) ASD GWAS;  $N_{\text{aut}} = 8,605$ ,  $N_{\text{nonaut}} = 19,526$ ) (53); for SCZ we chose the SCZ CLOZUK+PGC meta-analysis GWAS ( $N_{\text{aut}} = 40,675$ ,  $N_{\text{nonaut}} = 64,643$ ) (54); for BD we used the BD PGC GWAS ( $N_{\text{aut}} = 20,129$ ,  $N_{\text{nonaut}} = 21,524$ ) (55); for EA (number of years of schooling completed) we chose the SSGAC (Social Science Genetic Association Consortium) EA meta-analysis GWAS ( $N = 293,723$ ) (56). Variants of interest were those in each GWAS with  $MAF \leq 0.05$ , missingness per individual  $\leq 0.1$ , missingness per SNP = 0, Hardy-Weinberg Equilibrium  $\leq 1e^{-6}$ . Candidate variant weights were then generated by running LDpred (57). PGS models corresponding to increasing fractions of contributing causal SNPs (0.001, 0.003, 0.01, 0.03, 0.1, 0.3, 1, Inf) were computed. Then, we evaluated the produced PGS models for each phenotype for their prediction of ASD status, using sex and the first two genotype principal components, PC1 and PC2, as model covariates. We removed (regressed out) PC1 and PC2 from PGS for the final evaluation of each PGS association with ASD status. To choose the best model for each phenotype, we examined both its Nagelkerke's  $R^2$  and its regression coefficient for ASD status.

After examination, for all phenotypes of interest we chose the PGS model assuming that all SNPs were causal ( $p = 1$ ).

### *pTDT*

We used the polygenic transmission disequilibrium test (pTDT) (58) to determine whether an offspring's genetic predisposition for ASD was consistent with what is expected based on parental transmission of polygenic risk for ASD. We first calculated the mid-parent PGS ( $PGS_{MP}$ ) for the 1,519 children of European ancestry, using the following equation:

$$PGS_{MP} = \frac{PGS_{mother} + PGS_{father}}{2}$$

The  $PGS_{MP}$  was then used to compute the pTDT deviation for each child. The pTDT deviation is defined as follows:

$$pTDT_{deviation} = \frac{PGS_c - PGS_{MP}}{SD(PGS_{MP})}$$

where  $PGS_c$  is the PGS for the autistic or nonautistic child, and  $SD(PGS_{MP})$  is the standard deviation of the sample-specific mid-parent PGS. In order to determine if the pTDT deviation was significantly different from zero, the two-sided, one-sample *t*-test was conducted using the pTDT test statistic ( $t_{pTDT}$ ):

$$t_{pTDT} = \frac{mean(pTDT\ deviation)}{SD(pTDT\ deviation)\sqrt{n}}$$

where  $n$  is the number of families included in the pTDT study. The same strategy was used for testing overtransmission of PGS for SCZ, BD, and EA.

### **Phenotypic comparisons among children of AGRE multiplex families**

We used the available phenotypic data to (1) investigate the phenotypic effect of rare de novo (RDN) and rare inherited (RI) variants in the 152 KARGs and to (2) identify potential links between PGS overtransmission and phenotype severity through stratified pTDT based on children that do not carry any rare variant in the 74 TADA genes.

For the phenotypic distribution comparisons, we used data available for the 2,254 fully-phaseable children whereas, for the stratified pTDT analysis, we used those with phenotype available for the 1,519 fully-phaseable children of European ancestry.

For each phenotypic measure, we used (1) the corresponding standard hypothesized value, to which we compared the phenotypic distribution median value of each group of autistic children (stratified by those carrying RDN or RI variants in KARGs and those without such variants) and (2) cut-off value(s), for stratified pTDT analysis of autistic TADA ASD risk gene noncarriers.

IQ scores are normally distributed with a mean of 100 and a standard deviation of 15. We used the median value of 100 as the standard hypothesized value and a cut-off value of 70 (two standard deviations below the mean) to stratify children by those with (IQ < 70) or without (IQ ≥ 70) cognitive impairment.

To represent normal variation in age of walking (AOW), we used the window of achievement for the "walking alone" milestone observed in the normative cohort of the WHO Multicentre Growth Reference Study (MGRS) (59). Specifically, the 50<sup>th</sup> percentile estimate of 12 months derived from this window was used as the standard hypothesized value, whereas the 97<sup>th</sup>

percentile estimate of 16 months was used to divide children in those with delayed (AOW  $\geq$  16) or nondelayed (AOW < 16) motor development.

Nonautistic children were assessed for language development through the AGRE custom seven-item language questionnaire. For both language measures, ages of first word and phrase, we used the available data to build “nonautistic noncarrier” distributions representing the normal variation in milestone achievement among the nonautistic siblings. We used the median values of 12 months and 18 months from the “nonautistic noncarrier” distributions as reference hypothesized values for age of first word and age of first phrase, respectively. Both ADI-R items, age of first word and age of first phrase, are scored in section D of the diagnostic algorithm, with a score of 1 indicating that the age of milestone achievement suggests that developmental concerns are present at or before 36 months and a score of 0 denoting that the age of milestone achievement falls within the range of normal variation. Specifically, age of first word is scored as 1 if greater than 24 months; age of first phrase is scored as 1 if greater than 33 months. We used this scoring system to stratify children by those with delayed (score = 1) or nondelayed (score = 0) language development.

Total raw scores from SRS were available for both autistic and nonautistic children in AGRE. We used the scores available for the nonautistic noncarriers to build a reference distribution representing the normal variation in social behavior and social interaction skills. We used the median score of 19 derived from the “nonautistic noncarrier” distribution as reference hypothesized value for testing differences in SRS total raw scores. In addition, to stratify children based on their social skills, we computed corresponding T-scores using means, standard deviations, and sample sizes from the child’s sex-based school-age norm tables reported in the SRS manual (60). We used the following SRS T-score cut-off ranges to divide the autistic noncarriers into groups showing different degrees of social impairment: T-scores equal to 59 or less were considered as non-ASD, those among 60 and 75 as representative of mild ASD, and those equal to 76 or more as characteristic of severe ASD (61).

When data were collected using different version forms for the same assessment tool, we only used those coming from the most frequently used version form to ensure that form version did not drive potential phenotypic differences. An exception was made for SRS, for which we combined the compatible preschool and school-age forms.

When data for the same child were collected more than once, in more than one visit, we kept only those from the most recent visit for further analysis. Again, a different criterion was used for SRS. We removed data from assessments flagged as invalid. When valid SRS data for the same child were collected in more than one visit, (1) if both a parent and a teacher were available as corresponding respondents, the teacher-based assessment was preferred as more reliable, whereas (2) if the same respondent contributed to longitudinal assessments, the earliest visit data was used for downstream analysis (62). In addition, since SRS has not been validated in nonverbal children, we used the ADI-R item age of first word to identify children that had not reached or regained this milestone and we removed their entries from the SRS dataset (62). Finally, we computed sex-based T-scores only for autistic noncarriers with ages 4 to 18 years (school-age sample).

Many children in the cohort were still not able to walk or were nonverbal at the time of testing. In order to keep these informative observations for the analysis despite not having a numeric value for those cases, for those cases, we converted the codes for “milestone not reached” and “milestone lost and not regained yet” into the age of those children at the time of testing plus one month, optimistically assuming for them a potential milestone achievement soon after the latest assessment. Similarly, with the aim of not losing relevant information coming from Ravens data, we converted the codes for “below age-specific test norms” and “above age-specific test norms” nonverbal IQ scores into the cohort lowest minus one point and highest plus one point scores, respectively. There were two cases of autistic “double carrier” of both a RDN and a RI variant in KARGs and a case of autistic “double carrier” of variants in the TADA ASD risk

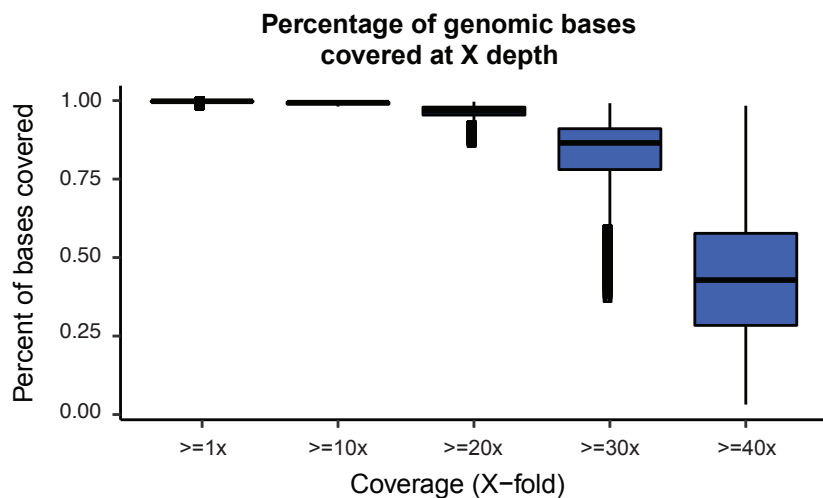
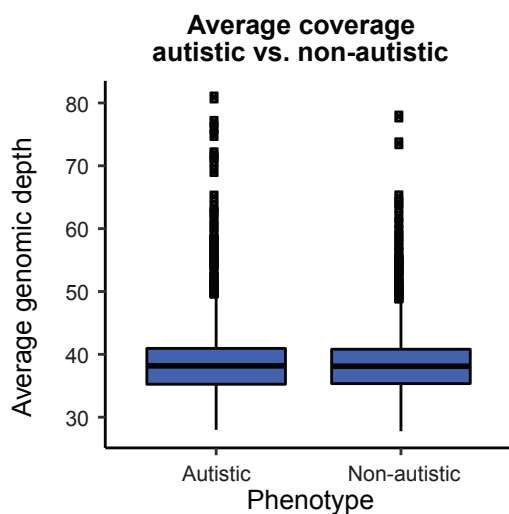
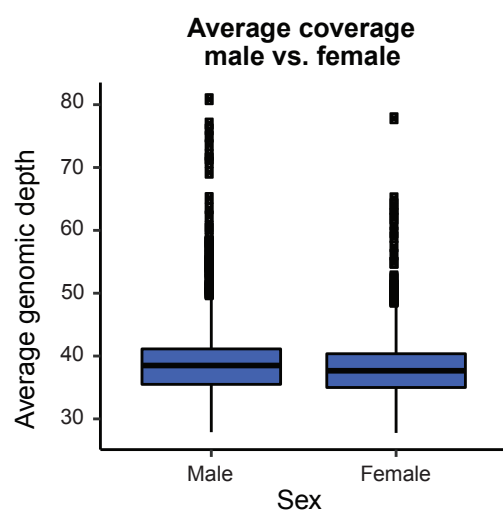
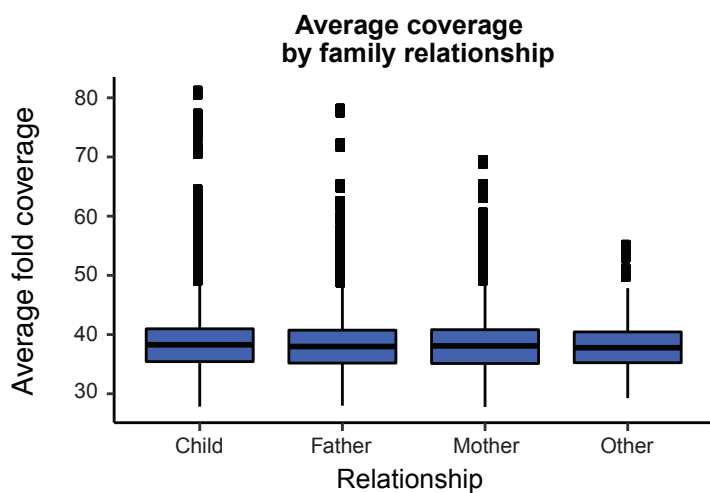
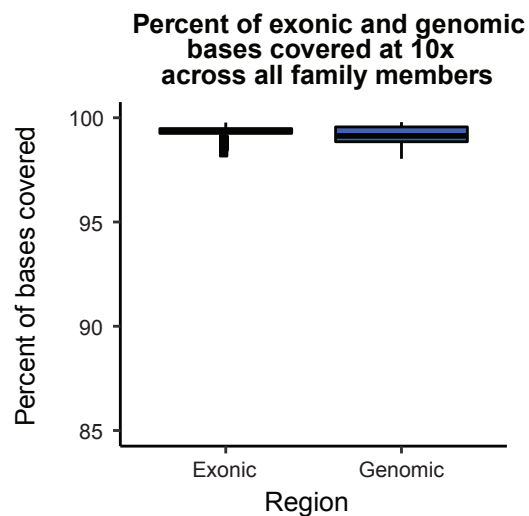
genes identified at  $FDR < 0.1$ . We decided to group these children as RDN carriers, assuming a larger effect size for de novo variants.

We excluded some specific groups of children from these phenotypic comparison analyses: autistic children with confirmed motor development impairment (cerebral palsy diagnosis), autistic children with seizures, nonautistic children with learning disabilities, nonautistic children with language disabilities, nonautistic children with previous and no longer confirmed ASD diagnosis, and nonautistic children carrying qualifying rare variants in KARGs and in the TADA ASD risk genes identified at  $FDR < 0.1$ . These children were removed with the idea of minimizing the potential confounding effect of comorbid phenotypes and ASD-associated genetic variation on the measures tested. Even though we had IQ scores available for very few nonautistic children we decided to remove them from the analyses, keeping them only on autistic children. We only used data from nonautistic children to build the ADI-R item and SRS total raw score “nonautistic noncarrier” distributions mentioned above.

Since the phenotypic measure distributions were not normal and asymmetric, we tested potential differences between their median values and standard hypothesized values through two-sided one-sample sign tests. The three tests performed for each phenotypic measure were considered as simultaneous multiple tests and we used the Benjamini and Hochberg (BH) procedure as FDR (false discovery rate)-controlling method. An  $FDR < 0.05$  was considered significant. For each measure, we tested for differences among the three autistic groups by a Kruskal-Wallis test and obtained non-significant results. For the phenotypic measure-stratified pTDT analysis, we compared the pTDT deviation distribution mean values against the expected value of 0 through two-sided one-sample  $t$ -tests. We defined a nominal  $p$ -value  $< 0.05$  as significant.

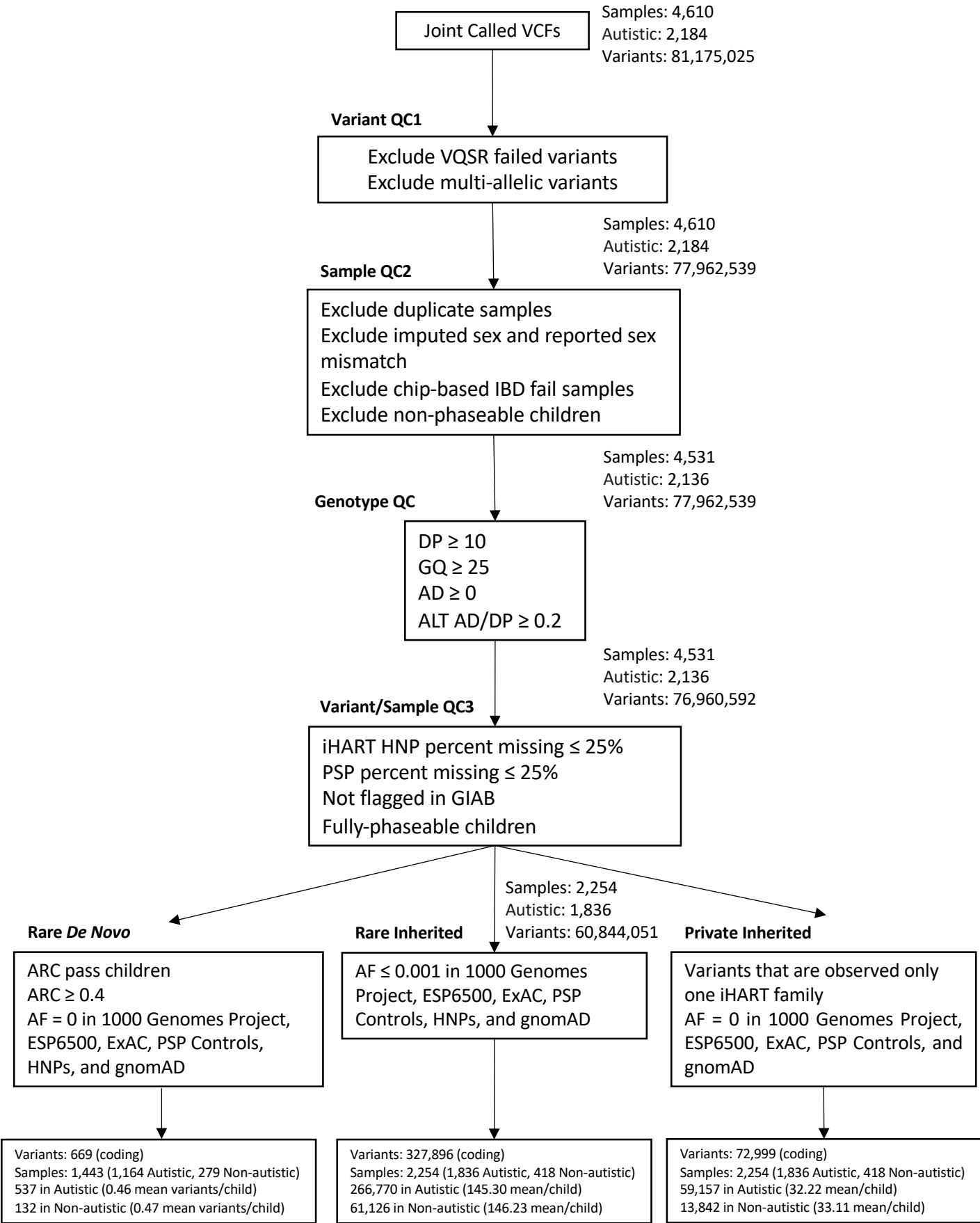
### **Quantification and statistical analysis**

Statistics were calculated using R (4.0.2) unless otherwise noted. The significance of PPI networks was evaluated using DAPPLE metrics based on 1,000 permutations (within the DAPPLE parameter);  $p$ -values  $> 0.05$  were considered significant.

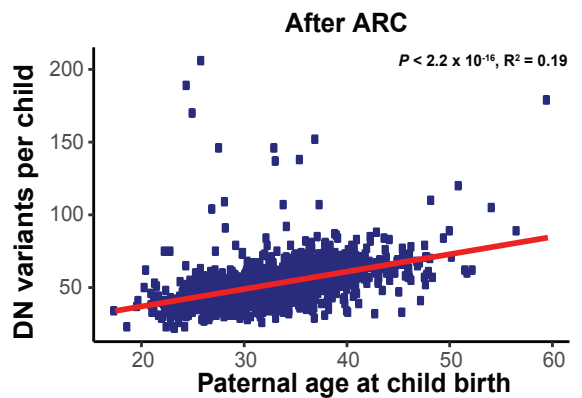
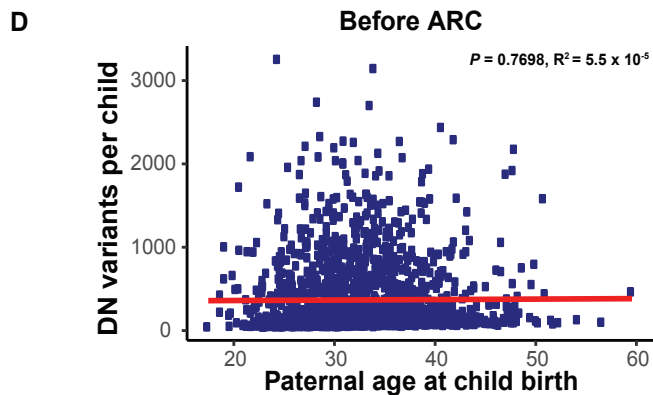
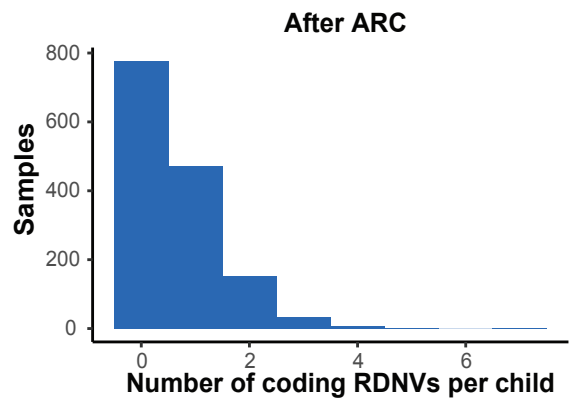
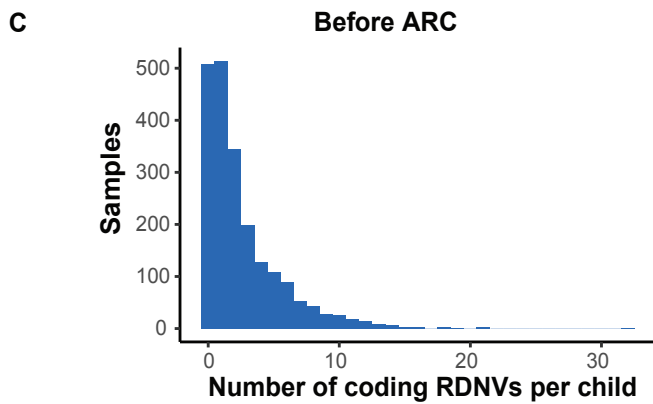
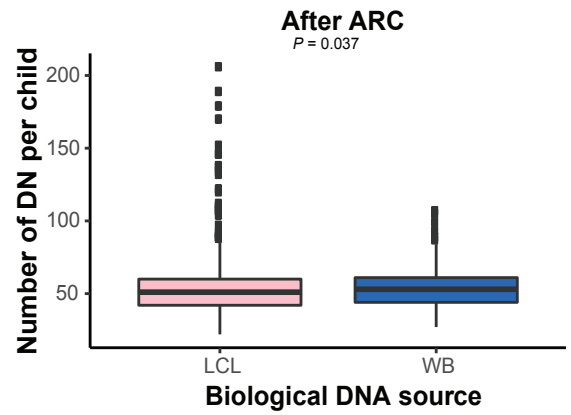
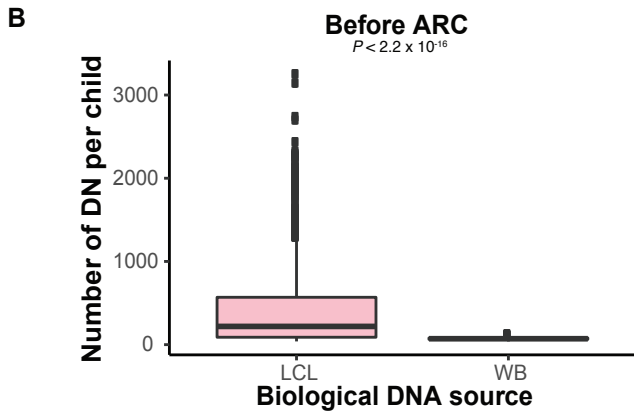
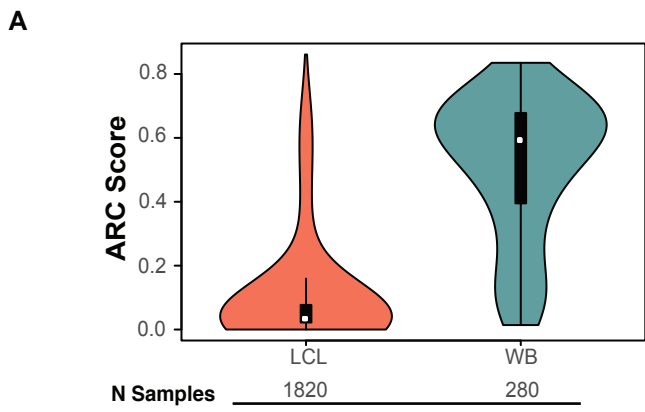
**A****B****C****D****E**



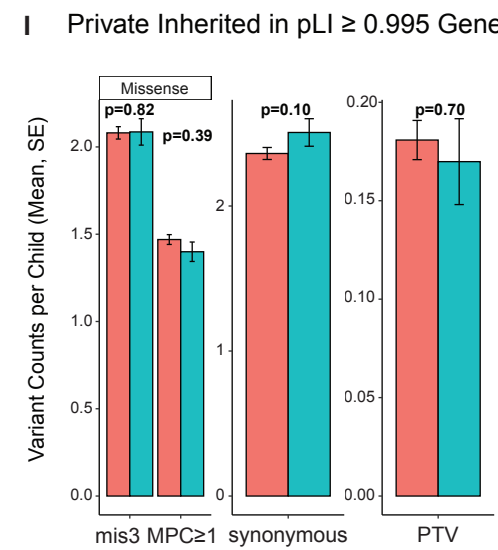
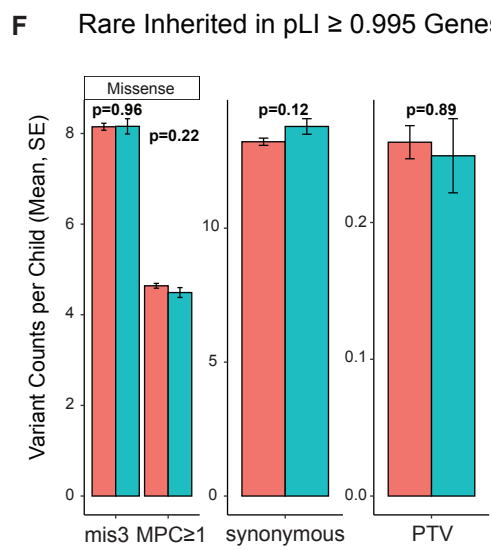
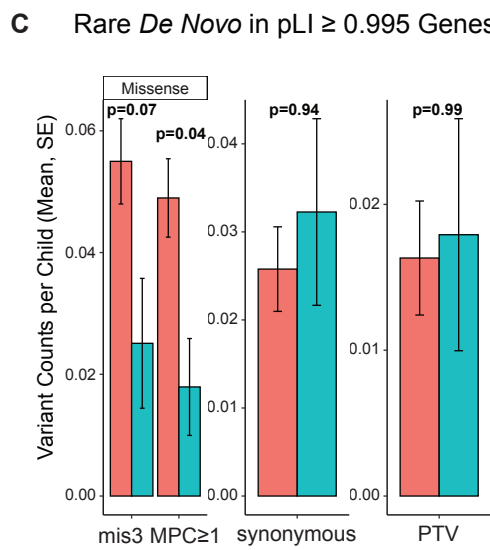
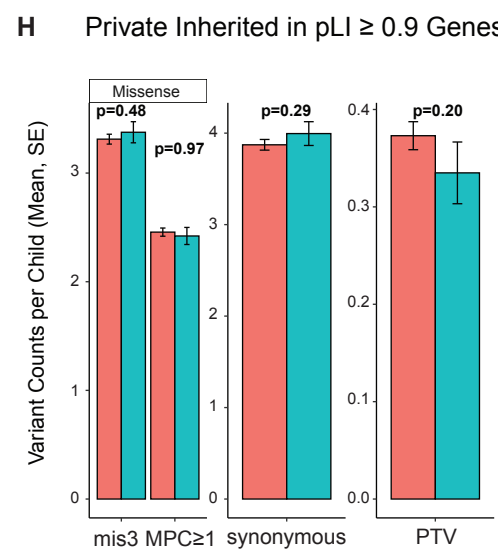
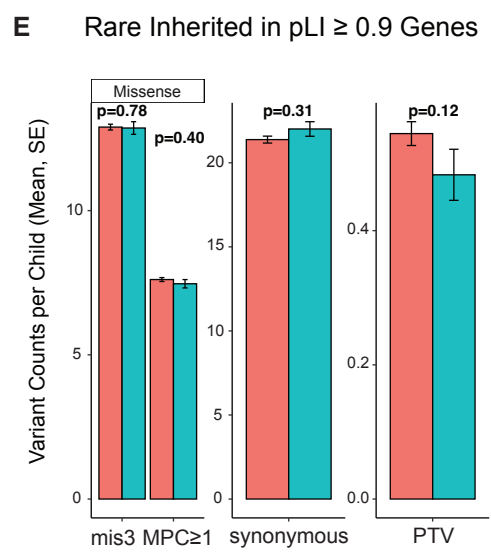
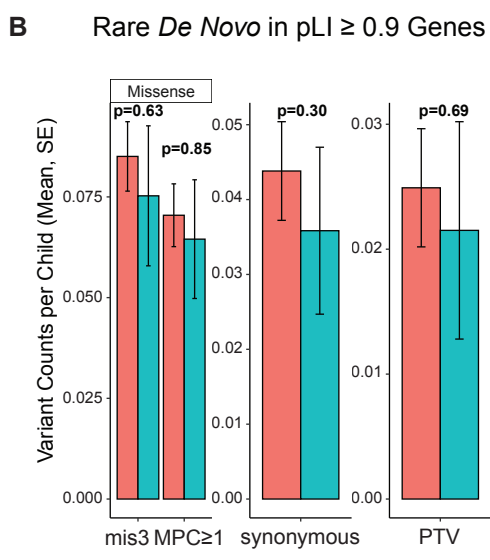
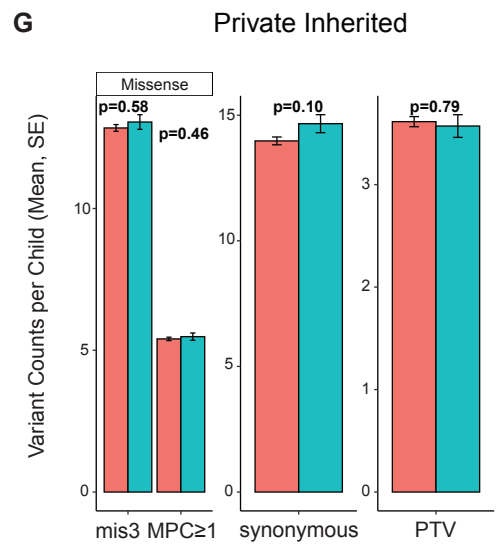
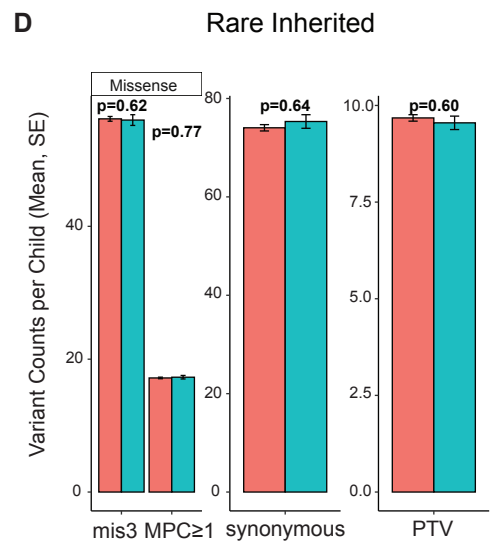
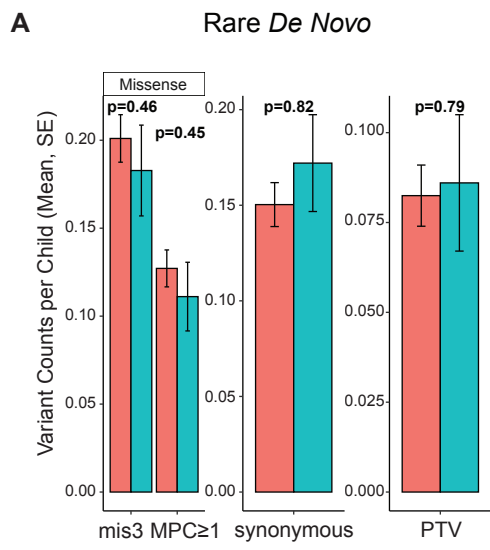
**Figure S1.** WGS coverage statistics for 4,551 AGRE multiplex family samples. (A) For the 4,551 samples with WGS data, the percent of genomic bases covered at 1X, 10X, 20X, 30X, and 40X bases is shown. On average,  $99.23 \pm 0.35\%$  (SD) of bases were covered at a depth of  $\geq 10X$ . The average fold coverage per sample across the cohort is shown with no differences in the categories of (B) ASD status, (C) sex, or (D) family member type – where family member type was categorized as either Child (proband, sibling, MZ or DZ twin), Father, Mother, or Other (e.g., cousin). (E) The percent of exonic and genomic bases covered at  $\geq 10x$  across all family members present in the 865 fully-phaseable AGRE multiplex families is shown. Exonic regions are those that are annotated as protein-coding exons ( $>75\text{MB}$ ) in Gencode V19. All non-N bases in the reference genome ( $>2.8\text{Gb}$ ) were considered genomic regions.



**Figure S2.** Whole-genome sequencing pipeline overview. An overview of the variant, sample, and genotype quality control conducted on the raw joint called variants to obtain the rare de novo, rare inherited, and private inherited variants used in downstream analyses. Abbreviations: VCF (Variant Call Format), QC (Quality Control), VQSR (Variant Quality Score Recalibration), IBD (Identity by Descent), DP (Read Depth), GQ (Genotype quality), AD (Allele Depth), HNP (Healthy Non-phaseable), PSP (Progressive Supranuclear Palsy), GIAB (Genome in a Bottle Consortium).

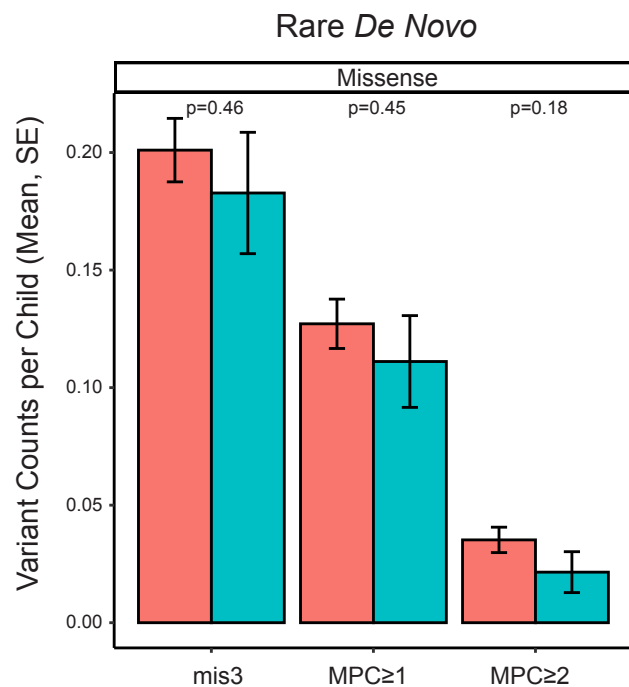
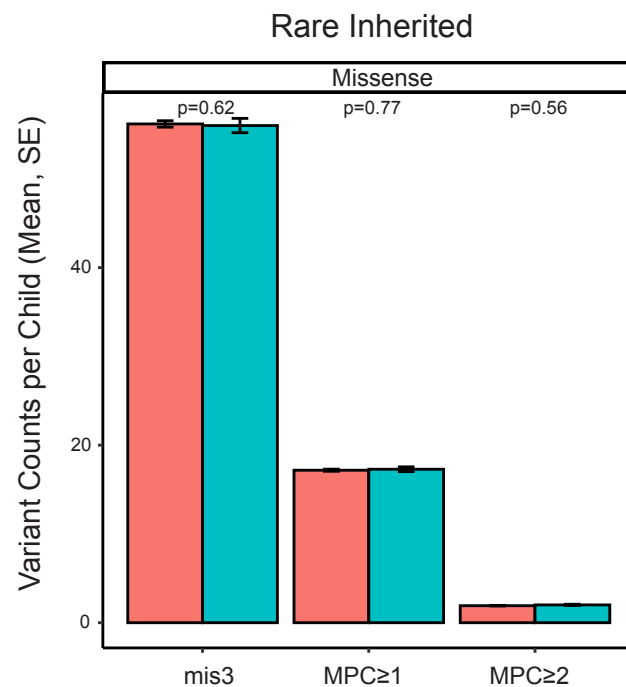
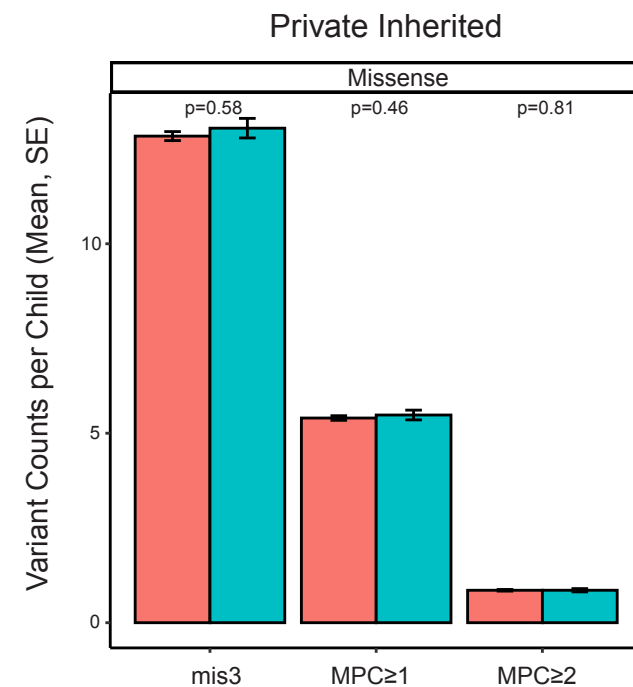
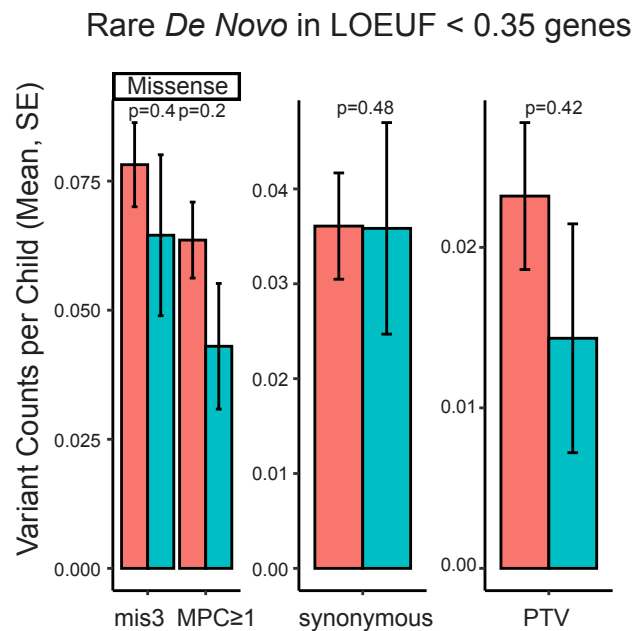
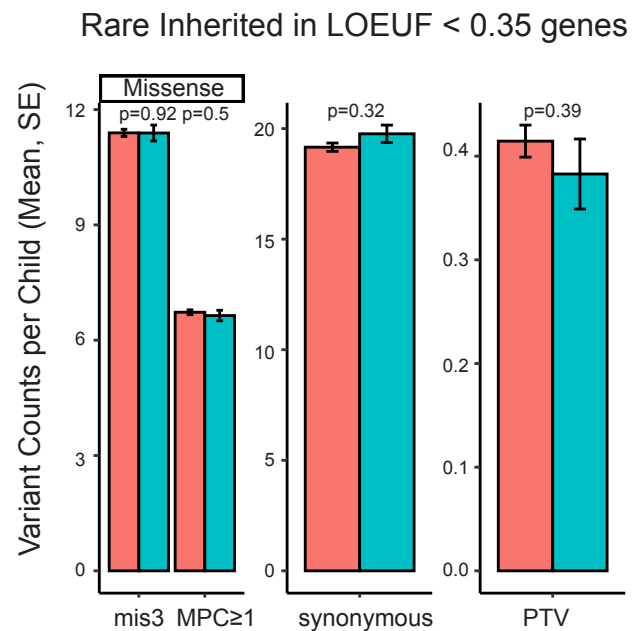
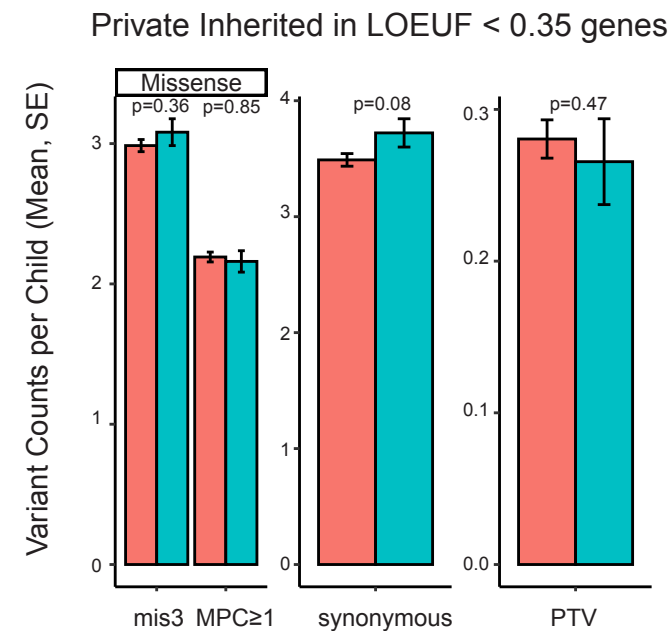


**Figure S3.** Rare de novo variants (RDNVs) in cohort samples before and after Artifact Removal by Classifier (ARC). (A) Distribution of RDNV ARC scores from 2,100 fully-phaseable non-monozygotic (MZ) twin samples. Red represents samples derived from lymphoblastic cell lines (LCL) and green represents samples derived from whole blood (WB). (B) In LCL (pink) and WB (blue) fully-phaseable (non-MZ twin) samples, the number of RDNVs identified per sample before ARC (N = 2,100 samples) and the number of RDNVs identified in LCL (pink) and WB (blue) fully-phaseable (non-MZ twin) samples after ARC (variants with an ARC score < 0.4 are filtered out) and after excluding ARC outlier samples (samples with >90% DNs removed by ARC) (n = 1,443). After ARC, there is a less significant difference in the rate of RDNVs based on the biological sequencing source (LCL mean = 52.6 and WB mean = 53.6; LCL median = 51 and WB median = 53). The Wilcoxon rank sum test was used to evaluate the difference in RDNV rates between the biological sequencing source (LCL versus WB). (C) Histograms displaying the number of coding RDNVs per fully-phaseable sample. Before ARC, coding RDNVs come from 2,100 fully-phaseable non-MZ twin samples; after ARC (which filters out variants with an ARC score < 0.4), variants are derived from samples excluding ARC outliers (samples with >90% DNs removed by ARC) and MZ twins (n = 1,443). (D) The correlation between paternal age and the rate of RDNVs before and after ARC. This analysis considers 1,677 fully-phaseable ASD children (excluding MZ twins) for which paternal age was known before ARC and 1,157 fully-phaseable ASD children (excluding MZ twins and ARC outliers) for which paternal age was known after ARC. The linear regression line is in red. On the left, the graph shows the number of raw RDNVs (SNVs and indels) per child by paternal age (years) at the time of the participant's birth. On the right, the graph shows the number of RDNVs (SNVs and indels) per child identified after running ARC by paternal age (years) at the time of the participant's birth.



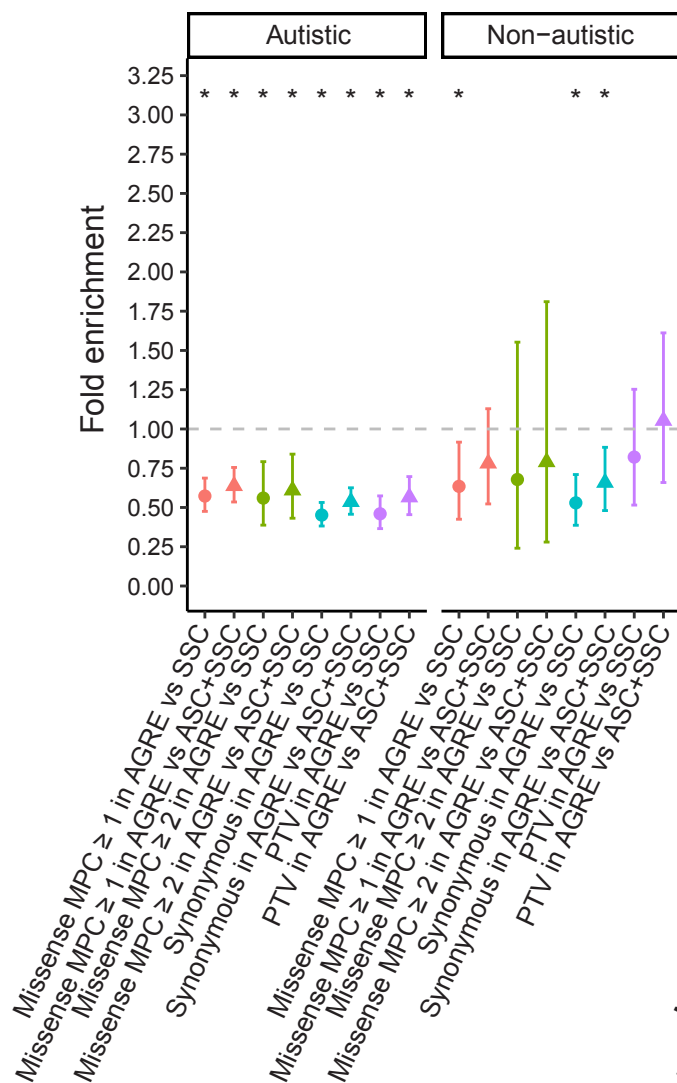
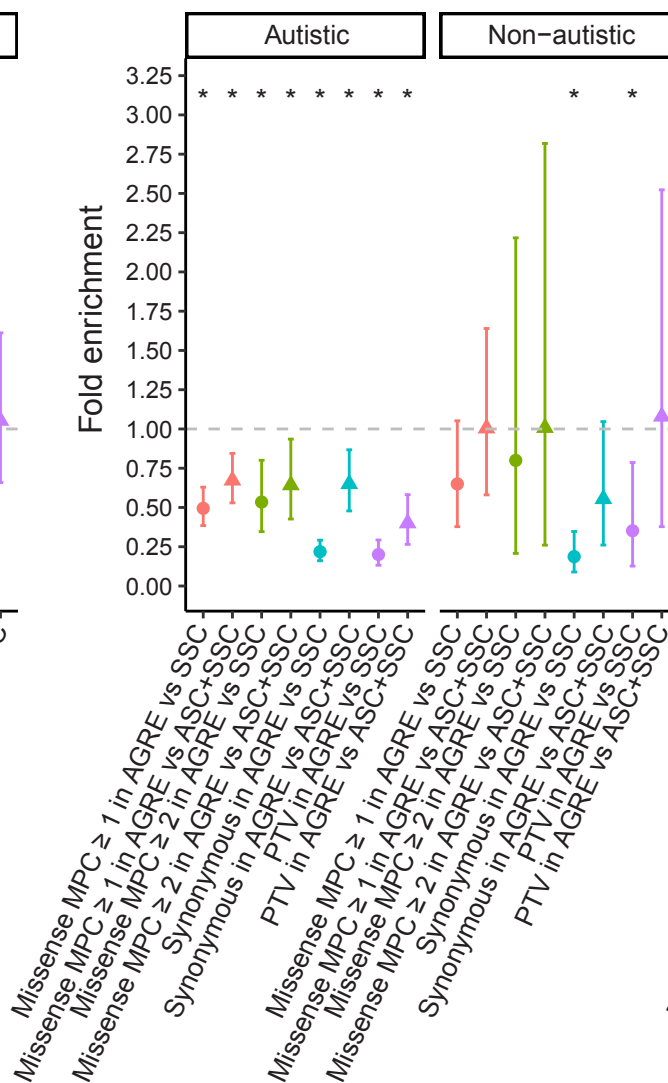
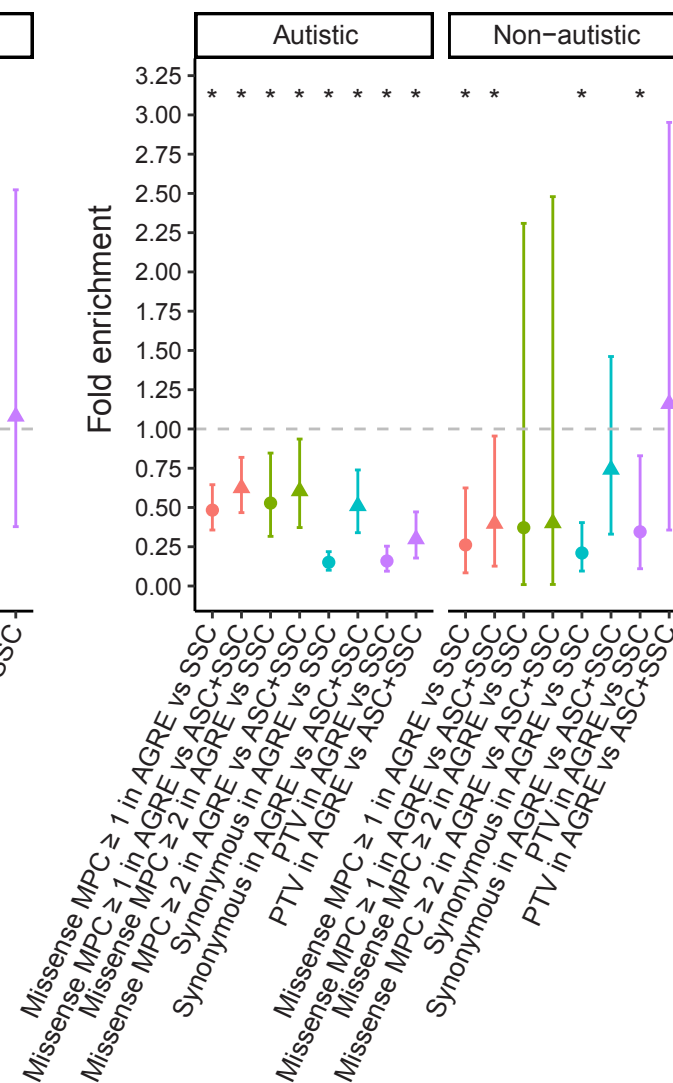
Phenotype ■ Autistic ■ Non-autistic

**Figure S4.** Coding variant rates in autistic (salmon) versus nonautistic (turquoise) fully-phaseable children. Mean  $\pm$  standard error variant count per child is shown. (A-C) Rate of rare de novo variants in all genes, genes with pLI  $\geq$  0.9, and genes with pLI  $\geq$  0.995 stratified by variant type. (D-F) Rate of rare inherited variants in all genes, genes with pLI  $\geq$  0.9, and genes with pLI  $\geq$  0.995 stratified by variant type. (G-I) Rate of private inherited variants in all genes, genes with pLI  $\geq$  0.9, and genes with pLI  $\geq$  0.995 stratified by variant type. mis3 = Polyphen-2 missense 3, MPC  $\geq$  1 = missense deleterious metric. (For rare and private inherited coding variants, fully-phaseable children include 2,254 children and for rare de novo coding variants analysis includes 1,443 non-ARC outlier children).

**A****B****C****D****E****F**Phenotype ■ Autistic ■ Non-autistic



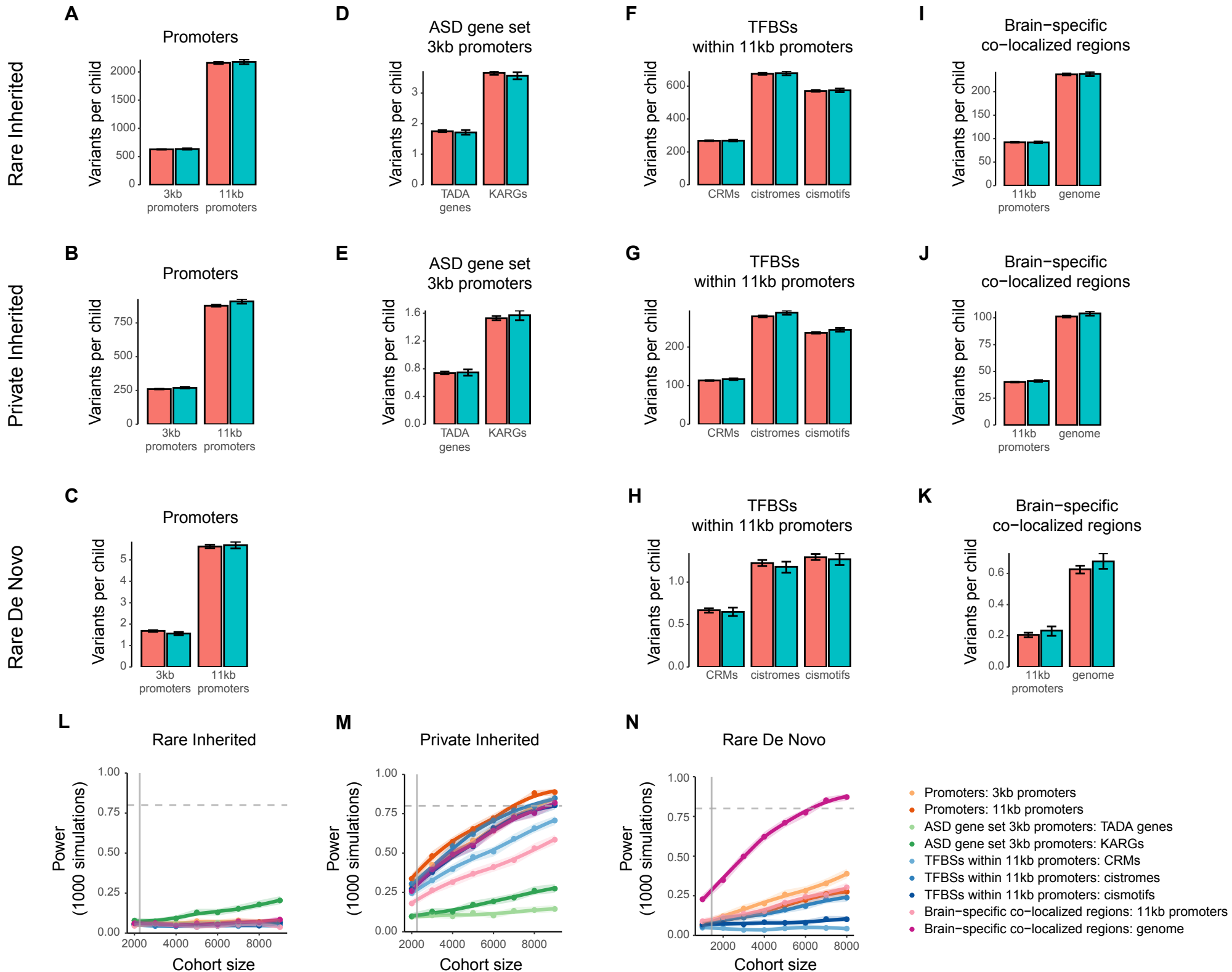
**Figure S5.** Coding variant rate comparison in autistic (salmon) versus nonautistic (turquoise) fully-phaseable children through additional functional annotation scores (MPC and LOEUF). Mean  $\pm$  standard error variant count per child is shown. (A-C) Rate of rare de novo, rare inherited, and private inherited missense variants defined by three different approaches: Polyphen-2 missense 3, MPC  $\geq$  1, and MPC  $\geq$  2. (D-F) Rate of rare de novo, rare inherited, and private inherited variants in constrained genes defined by LOEUF score  $<$  0.35.

**A****All genes****B****pLI  $\geq 0.9$  genes****C****pLI  $\geq 0.995$  genes**

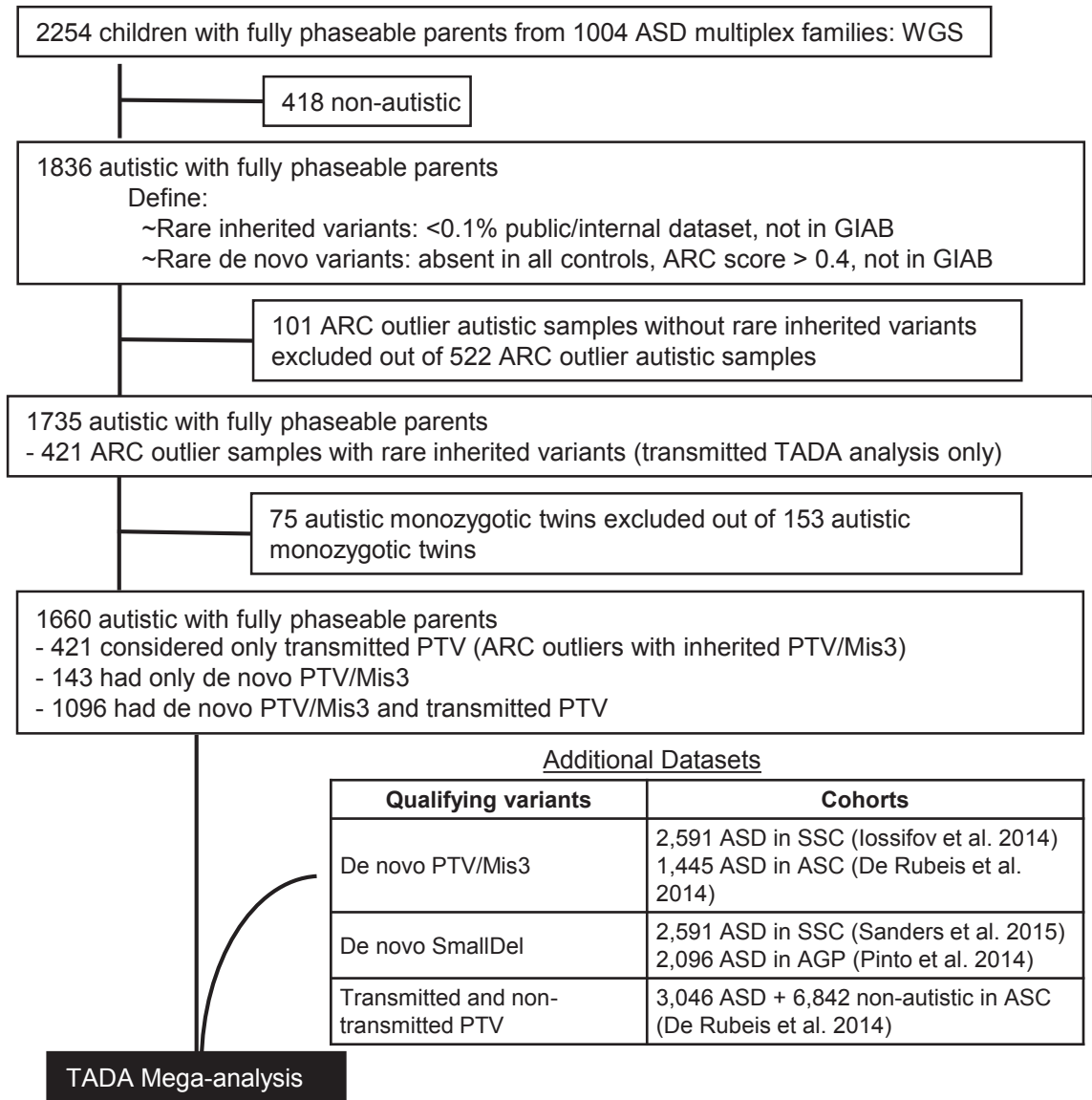
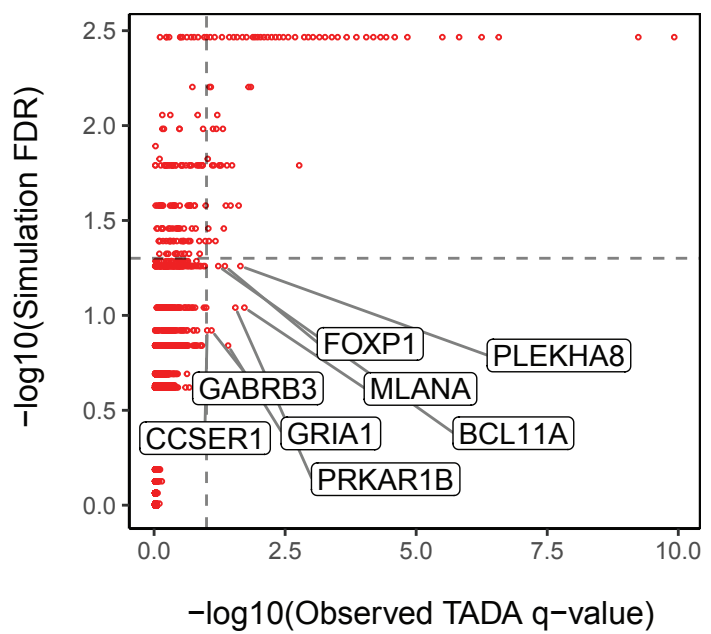
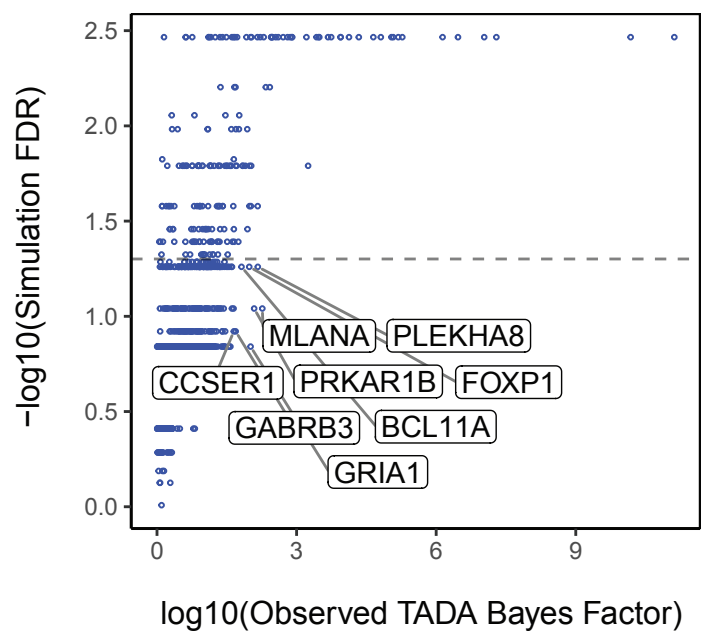
Cohort de novo variant rate comparison ● AGRE vs SSC (Zhou 2022) ▲ AGRE vs ASC+SSC (Fu 2022)

De novo variant set ● Missense MPC  $\geq 1$  ● Missense MPC  $\geq 2$  ● Synonymous ● PTV

**Figure S6.** Depletion of rare de novo coding variation in AGRE multiplex families compared to ASD simplex family-based collections. Observed rates of de novo missense variants ( $MPC \geq 1$  and  $MPC \geq 2$ ), synonymous variants, and PTVs in (A) all genes, (B)  $pLI \geq 0.9$  genes, and (C)  $pLI \geq 0.995$  genes are compared in AGRE versus SSC (2) (circles) and in AGRE versus ASC+SSC (3) (triangles). Each y-axis reports the variant set fold enrichment, or rate ratio, in AGRE compared to the other two simplex-based collections. 95% confidence intervals are shown as error bars. Asterisks indicate Poisson test p-values  $< 0.05$  (Dataset S5). Autistic: 1,164 for AGRE; 2,654 for SSC; 8,028 for ASC+SSC. Nonautistic: 279 for AGRE; 2,176 for SSC; 2,460 for ASC+SSC.



**Figure S7.** Noncoding variation in AGRE multiplex family children. (A-K) Number of noncoding variants per fully-phaseable child in autistic (salmon) and nonautistic (turquoise) children. Mean  $\pm$  standard error variant count per child is shown. (A-C) For promoter regions, rare inherited noncoding variants in 1,836 autistic versus 418 nonautistic children (A), private inherited noncoding variants in 1,836 autistic versus 418 nonautistic children (B), and rare de novo noncoding variants in 1,164 autistic versus 279 nonautistic children (C). (D-E) For promoter regions of ASD risk genes, rare inherited noncoding variants in autistic versus nonautistic children (D), and private inherited noncoding variants autistic versus nonautistic children (E). (F-H) For transcription factor binding sites (TFBSs) in promoter regions, rare inherited noncoding variants in autistic versus nonautistic children (F), private inherited noncoding variants autistic versus nonautistic children (G), and rare de novo noncoding variants in autistic versus nonautistic children (H). (I-K) For brain-specific colocalized regions, rare inherited noncoding variants in autistic versus nonautistic children (I), private inherited noncoding variants in autistic versus nonautistic children (J), and rare de novo noncoding variants in autistic versus nonautistic children (K). (L-N) Curves showing power at increasing sample sizes for the quantitative burden testing through logistic regression of rare inherited (L), private inherited (M), and rare de novo (N) noncoding variants. Each curve corresponds to a tested variant set (see color-coded legend), with individual points representing power values specific to the “variant count per child” predictor, computed based on 1,000 simulations, for the observed ASD odds ratio (OR) and at specific sample sizes. 95% confidence intervals for these power values are depicted as ribbons. The dashed grey horizontal line marks the 0.8 standard threshold used for power while the solid grey vertical line shows the current sample size for the specific variant set (2,254 fully-phaseable children for rare and private inherited noncoding variants and 1,443 children for rare de novo noncoding variants).

**A****B****C**

**Figure S8.** Rare variant TADA pre-processing and results from TADA simulations. (A) Detailed overview of cohort subjects and additional datasets included in the TADA analysis. Initial dataset included 2,254 children with fully-phaseable parents from 1,004 AGRE ASD multiplex families. Subjects were removed if they were nonautistic, were considered ARC outliers or were a monozygotic twin. Subsets of the 1660 autistic children were included in TADA for de novo or inherited analysis. Additional datasets used for TADA mega-analysis are shown. (B) Observed FDR from TADA mega-analysis is plotted against the FDR from 100,000 simulations for all the 18,472 genes that were part of the TADA analysis. Vertical dashed line represents q-value threshold of 0.1; horizontal dashed line marks simulation FDR threshold of 0.05. Labels are shown for 8 TADA genes (q-value < 0.1) with simulation FDR > 0.05. (C) For genes with Bayes factor (BF) > 1, the observed BF from TADA mega-analysis is plotted against the FDR from 100,000 simulations. Refer to panel B legend for details about horizontal dashed line and point labels.

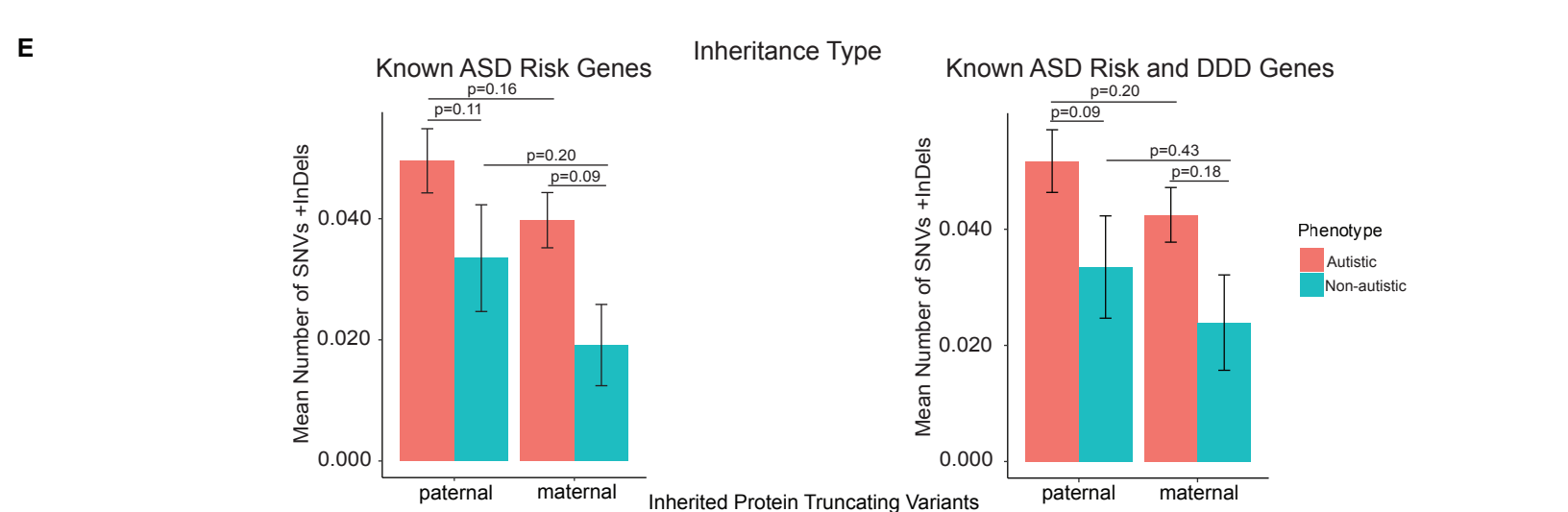
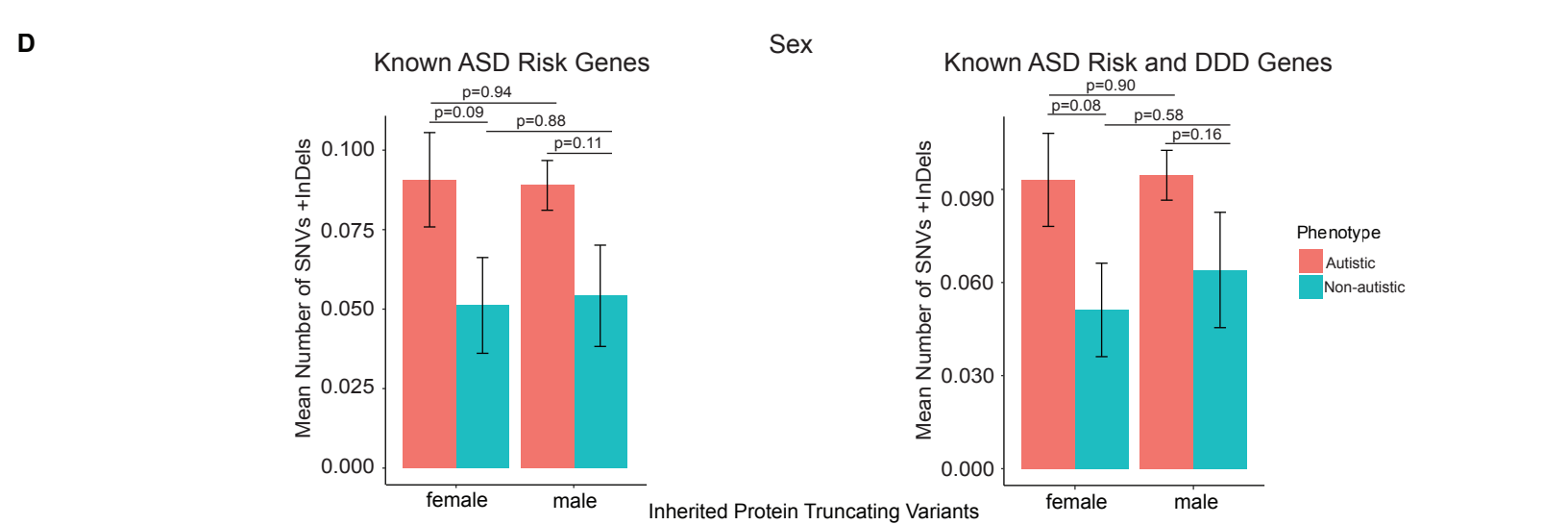
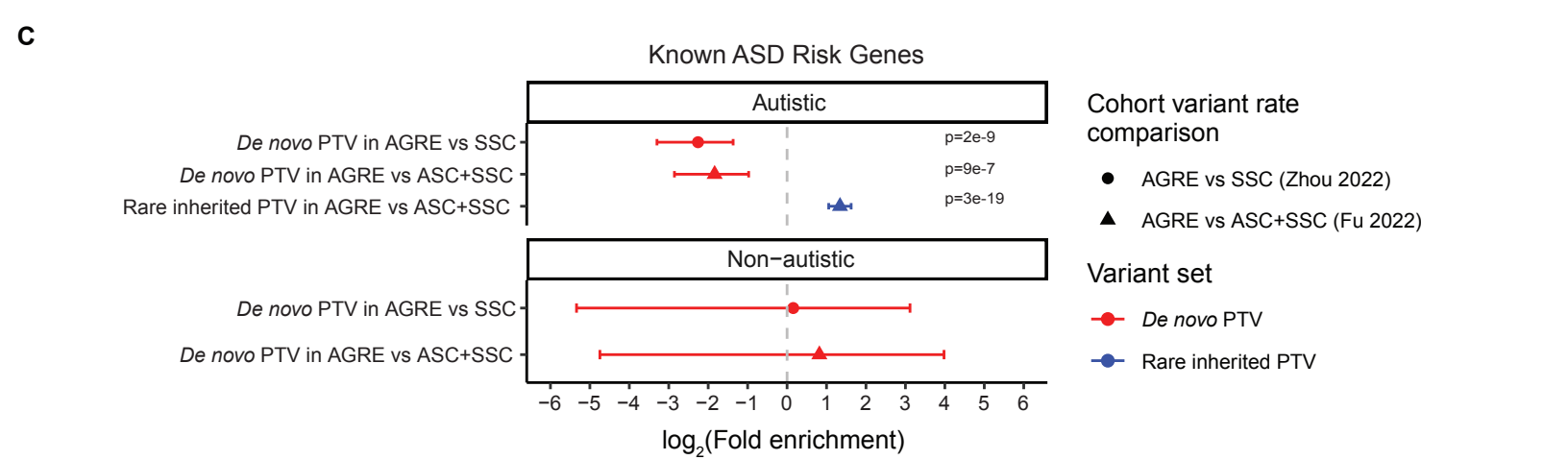
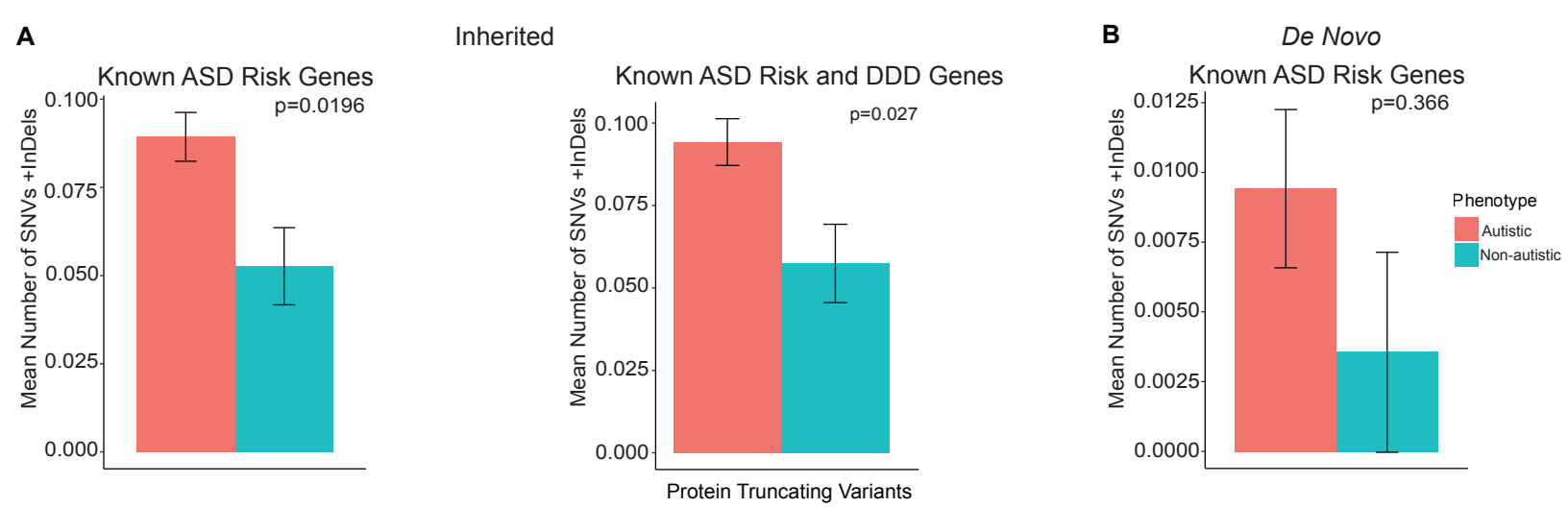
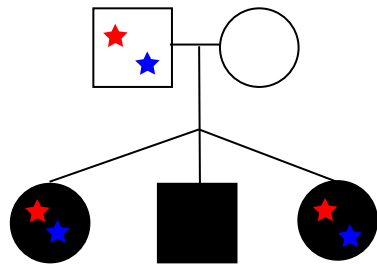
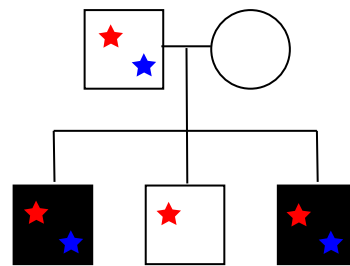




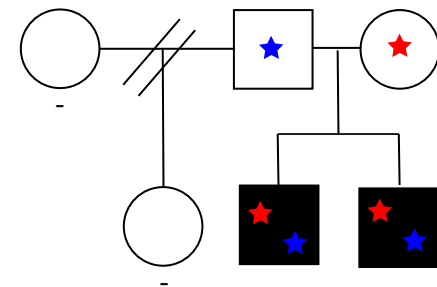
**Figure S9.** Known ASD risk gene variant rates, and known ASD and developmental disorder risk gene variant rates. (A-B) Mean  $\pm$  standard error number of protein truncating variants in autistic (salmon) versus nonautistic (turquoise) fully-phaseable children with inherited (A) and de novo (B) variants. (C) Depletion of rare de novo PTVs and enrichment of rare inherited PTVs in known ASD risk genes (KARGs) in AGRE multiplex families compared to ASD simplex family-based collections. Observed rates of de novo PTVs in KARGs (in red) are compared in AGRE versus SSC (2) (circles) and in AGRE versus ASC+SSC (3) (triangles). Observed rates of rare inherited PTVs in KARGs (in blue) are compared just for autistic children in AGRE versus ASC+SSC (3) (triangles). The x-axis reports the  $\log_2$  variant set fold enrichment, or rate ratio, in AGRE compared to the other two simplex-based collections. 95% confidence intervals are shown as error bars. Significant p-values from Poisson tests are reported (Dataset S5). Autistic: 1,164 for AGRE de novo; 1,836 for AGRE rare inherited; 2,654 for SSC; 8,028 for ASC+SSC. Nonautistic: 279 for AGRE; 2,176 for SSC; 2,460 for ASC+SSC. (D-E) Mean  $\pm$  standard error number of inherited protein truncating variants in autistic versus nonautistic fully-phaseable children stratified by sex (D) and inheritance type (E). For rare inherited variants, fully-phaseable children include 2,254 children and for rare de novo variants analysis includes 1,443 non-ARC outlier children.



AGRE multiplex family A  
 RANBP17  
 WDFY3



AGRE multiplex family B  
 CAPN12  
 FBXL13



AGRE multiplex family C  
 MFRP  
 SHANK3

- Not sequenced individual

**Figure S10.** Pedigrees of three cohort families in which two autistic children inherited the same pair of rare inherited PTVs in two known ASD risk genes from their nonautistic parents.

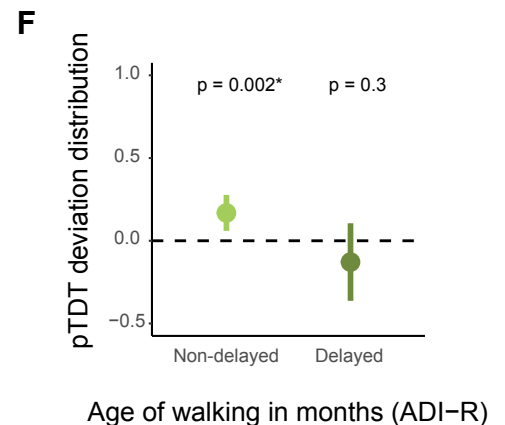
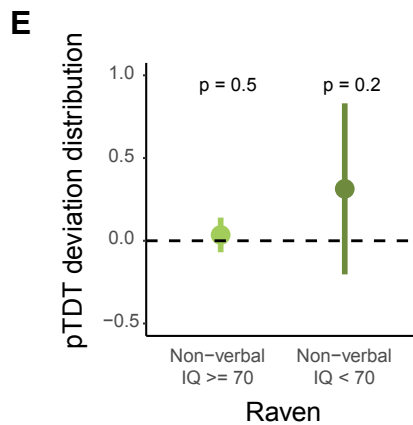
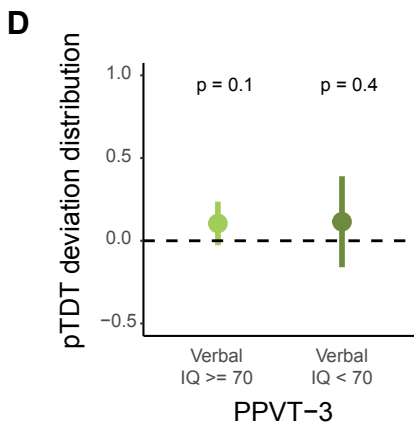
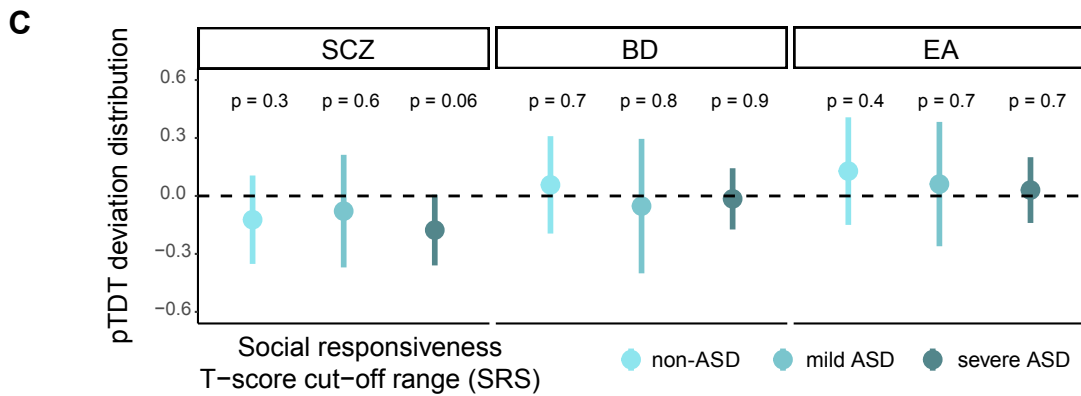
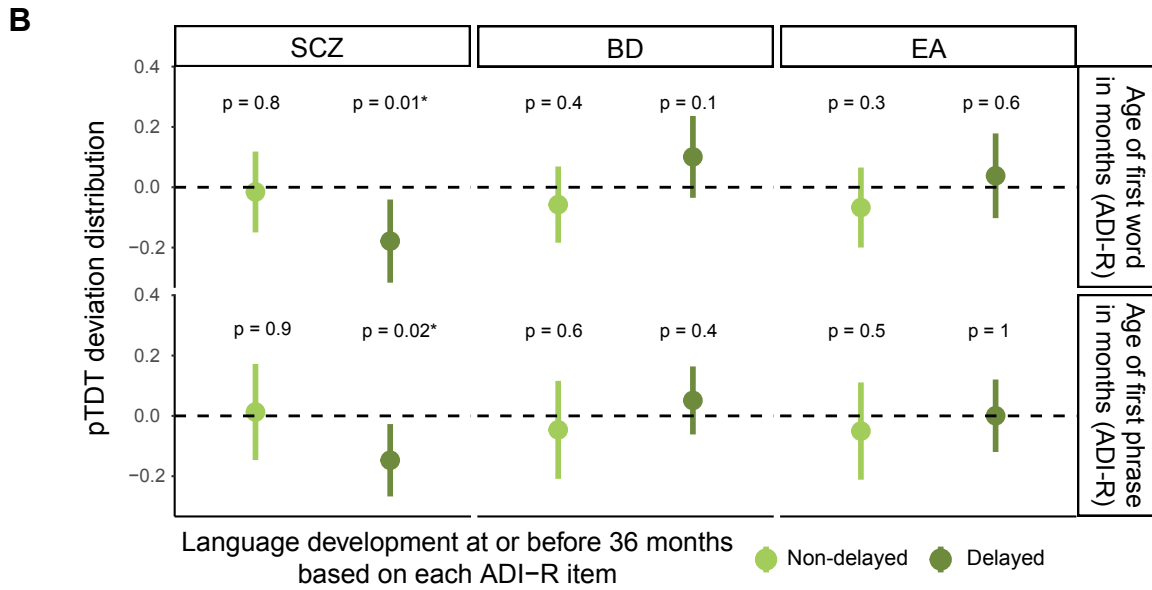
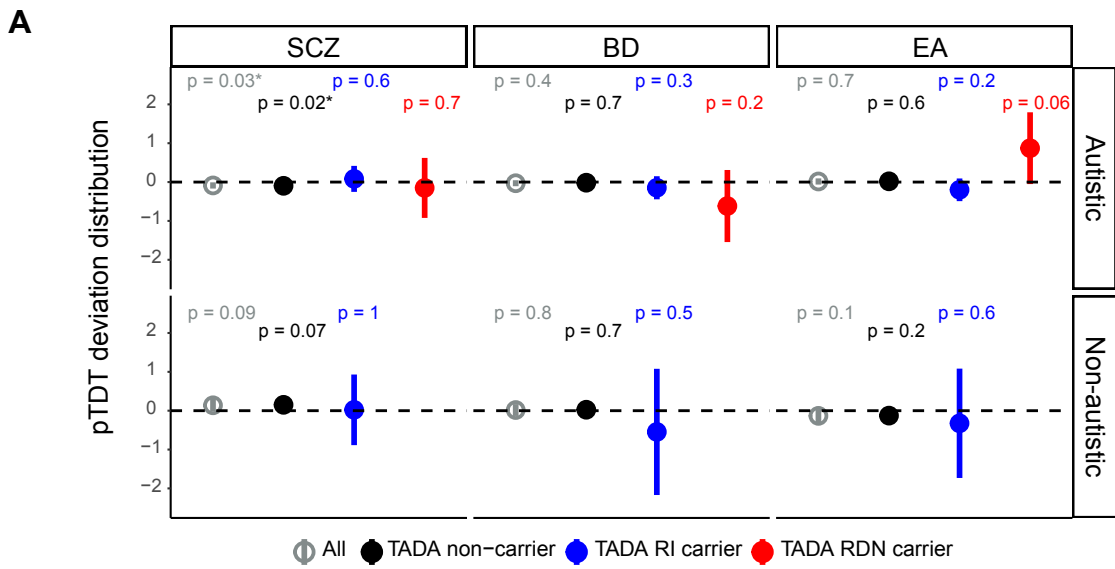


**Figure S11.** PGS for schizophrenia (SCZ), bipolar disorder (BD), and educational attainment (EA) in AGRE ASD multiplex families and ASD pTDT stratified by cognitive and motor impairment. (A) pTDT for SCZ, BD, and EA in autistic and nonautistic children, tested all together (All - autistic:  $n = 1231$ ; nonautistic:  $n = 288$ ) and stratified by those carrying rare inherited (TADA RI carrier - autistic:  $n = 70$ ; nonautistic:  $n = 8$ ) or rare de novo (TADA RDN carrier - autistic:  $n = 12$ ) variants in the TADA ASD risk genes identified at  $FDR < 0.1$  and those without such variants (noncarriers - autistic:  $n = 1149$ ; nonautistic:  $n = 279$ ). SCZ All - autistic:  $P = 0.03$ , pTDT deviation mean =  $-0.087$ . SCZ noncarriers - autistic:  $P = 0.02$ , pTDT deviation mean =  $-0.097$ . (B) pTDT for SCZ, BD, and EA in autistic noncarriers of variants in the TADA ASD risk genes identified at  $FDR < 0.1$  stratified by those with delayed (age of first word:  $n = 407$ ; phrase:  $n = 564$ ) language development (i.e., age of first word and phrase greater than 24 and 33 months, respectively; SI Appendix) and those with nondelayed (age of first word:  $n = 432$ ; phrase:  $n = 275$ ) language development. SCZ delayed age of first word:  $P = 0.01$ , pTDT deviation mean =  $-0.18$ . SCZ delayed age of first phrase:  $P = 0.02$ , pTDT deviation mean =  $-0.15$ . (C) pTDT for SCZ, BD, and EA in autistic noncarriers of variants in the TADA ASD risk genes identified at  $FDR < 0.1$  stratified by the degree of social impairment based on SRS (Social Responsiveness Scale) T-score cut-off ranges. T-scores (based on child's sex) equal to 59 or less were considered as non-ASD ( $n = 122$ ), those 60 to 75 were considered mild ASD ( $n = 70$ ), and those equal to or greater than 76 were considered severe ASD ( $n = 275$ ) (61). (D-E) pTDT for ASD in autistic noncarriers of variants in the TADA ASD risk genes identified at  $FDR < 0.1$  stratified by those with ( $IQ < 70$ ) or without ( $IQ \geq 70$ ) cognitive impairment, based on their verbal IQ scores from PPVT-3 (Peabody Picture Vocabulary Test, 3rd edition) (D) and nonverbal IQ ones from the Raven test (E). Verbal  $IQ \geq 70$ :  $n = 430$ ; Verbal  $IQ < 70$ :  $n = 106$ ; Nonverbal  $IQ \geq 70$ :  $n = 682$ ; Nonverbal  $IQ < 70$ :  $n = 39$ . (F) pTDT for ASD in autistic noncarriers of variants in the TADA ASD risk genes identified at  $FDR < 0.1$  stratified by those with nondelayed (age of walking in months  $< 16$ ,  $n = 669$ ) or delayed (age of walking in months  $\geq 16$ ,  $n = 135$ ) motor development. The age of 16 months chosen for stratification is the 97<sup>th</sup> percentile estimate for milestone achievement age in the normative cohort of the WHO Multicentre Growth Reference Study (MGRS) (59). Nondelayed motor development:  $P = 0.002$ , pTDT deviation mean =  $0.17$ . Polygenic transmission disequilibrium is shown on the y-axis of each panel as point ranges of the standard deviation on the mid-parent distribution mean values together with their 95% confidence intervals. The probability of each pTDT deviation distribution mean being equal to zero was tested by two-sided one-sample  $t$ -test. An asterisk is used to denote a  $p$ -value  $< 0.05$ . More details provided in the SI Methods section.

**Table S1.** Results from noncoding variant quantitative burden testing through logistic regression

Noncoding variant set			Set size	Logit model p	Variant count p	Variant count OR	Sex p	Sex OR	DNA source p	DNA source OR
Rare Inherited	Promoters	3kb promoters	1418044	1.0E-27	0.81	1	1.7E-29	0.281	0.2	0.813
		11kb promoters	4876012	1.0E-27	0.87	1	1.6E-29	0.28	0.2	0.813
	ASD gene set 3kb promoters	TADA genes	3933	1.0E-27	0.81	1.009	1.6E-29	0.28	0.2	0.815
		KARGs	8212	8.9E-28	0.57	1.014	1.6E-29	0.281	0.21	0.816
	TFBSs within 11kb promoters	CRMs	604207	1.0E-27	0.99	1	1.5E-29	0.28	0.2	0.813
		cistromes	1523034	1.0E-27	0.91	1	1.5E-29	0.28	0.2	0.813
		cismotifs	1288001	1.0E-27	0.9	1	1.5E-29	0.28	0.2	0.813
	Brain-specific colocalized regions	11kb promoters	208239	1.0E-27	0.93	1	1.5E-29	0.28	0.2	0.814
		genome	534567	1.0E-27	0.82	1	1.5E-29	0.28	0.2	0.813
	Private Inherited	Promoters	3kb promoters	591013	3.6E-28	0.14	0.999	2.1E-29	0.281	0.2
11kb promoters			1992171	2.9E-28	0.11	1	2.0E-29	0.281	0.2	0.814
ASD gene set 3kb promoters		TADA genes	1667	9.6E-28	0.67	0.974	1.4E-29	0.28	0.19	0.811
		KARGs	3462	8.3E-28	0.5	0.973	1.4E-29	0.28	0.19	0.811
TFBSs within 11kb promoters		CRMs	257009	4.8E-28	0.21	0.998	1.8E-29	0.281	0.2	0.815
		cistromes	634310	3.4E-28	0.13	0.999	1.9E-29	0.281	0.2	0.815
		cismotifs	537352	3.8E-28	0.15	0.999	1.9E-29	0.281	0.2	0.815
Brain-specific colocalized regions		11kb promoters	90740	5.8E-28	0.27	0.996	1.5E-29	0.28	0.2	0.814
		genome	229286	3.9E-28	0.15	0.998	1.4E-29	0.28	0.2	0.815
Rare De novo		Promoters	3kb promoters	2394	1.9E-14	0.5	1.035	7.4E-16	0.325	0.38
	11kb promoters		8138	1.9E-14	0.55	0.985	3.5E-16	0.322	0.36	0.859
	TFBSs within 11kb promoters	CRMs	959	2.3E-14	0.98	1.002	4.3E-16	0.323	0.37	0.86
		cistromes	1753	2.0E-14	0.58	1.034	4.0E-16	0.322	0.37	0.86
		cismotifs	1858	2.2E-14	0.76	1.018	3.9E-16	0.322	0.37	0.86
	Brain-specific colocalized regions	11kb promoters	305	1.9E-14	0.54	0.919	4.6E-16	0.323	0.37	0.861
		genome	919	9.6E-15	0.18	0.895	2.6E-16	0.319	0.34	0.853

For each noncoding variant set tested, total number of variants, significance of the logistic regression model built, and significance and ASD odds ratio (OR) for the three model predictors (variant count per child, child sex, and sample source of DNA used for whole-genome sequencing) are shown. Male sex and lymphoblastoid cell line (LCL) sample source of DNA were used as reference values for the two categorical variables. ASD OR for the variant count per child predictor represents the change in ASD odds for one unit increase of variant count per child.

**Table S2.** Results from power analysis for noncoding variant quantitative burden testing through logistic regression

Noncoding variant set			simr powerSim() function power	“sample” custom function power	“random” custom function power
Rare Inherited	Promoters	3kb promoters	0.06 (0.05, 0.08)	0.06 (0.04, 0.07)	0.06 (0.05, 0.08)
		11kb promoters	0.05 (0.03, 0.06)	0.06 (0.05, 0.08)	0.06 (0.04, 0.07)
	ASD gene set 3kb promoters	TADA genes	0.05 (0.04, 0.07)	0.06 (0.05, 0.08)	0.06 (0.05, 0.08)
		KARGs	0.09 (0.07, 0.11)	0.07 (0.05, 0.09)	0.09 (0.08, 0.11)
	TFBSs within 11kb promoters	CRMs	0.05 (0.04, 0.07)	0.04 (0.03, 0.05)	0.05 (0.04, 0.07)
		cistromes	0.05 (0.04, 0.07)	0.05 (0.04, 0.06)	0.06 (0.05, 0.08)
		cismotifs	0.04 (0.03, 0.06)	0.05 (0.04, 0.07)	0.07 (0.05, 0.08)
	Brain-specific colocalized regions	11kb promoters	0.05 (0.04, 0.06)	0.04 (0.03, 0.06)	0.07 (0.05, 0.08)
		genome	0.05 (0.04, 0.07)	0.05 (0.04, 0.07)	0.07 (0.05, 0.09)
	Private Inherited	Promoters	3kb promoters	0.33 (0.3, 0.36)	0.32 (0.29, 0.35)
11kb promoters			0.38 (0.35, 0.41)	0.38 (0.35, 0.41)	0.36 (0.33, 0.39)
ASD gene set 3kb promoters		TADA genes	0.07 (0.05, 0.09)	0.08 (0.06, 0.09)	0.07 (0.05, 0.08)
		KARGs	0.1 (0.09, 0.12)	0.12 (0.1, 0.14)	0.1 (0.08, 0.12)
TFBSs within 11kb promoters		CRMs	0.25 (0.22, 0.28)	0.26 (0.23, 0.28)	0.23 (0.21, 0.26)
		cistromes	0.33 (0.3, 0.36)	0.35 (0.32, 0.38)	0.32 (0.29, 0.35)
		cismotifs	0.29 (0.26, 0.32)	0.3 (0.27, 0.33)	0.31 (0.28, 0.34)
Brain-specific colocalized regions		11kb promoters	0.2 (0.18, 0.23)	0.2 (0.17, 0.22)	0.19 (0.17, 0.22)
		genome	0.31 (0.28, 0.34)	0.3 (0.27, 0.33)	0.29 (0.26, 0.32)
Rare De novo		Promoters	3kb promoters	0.1 (0.08, 0.12)	0.1 (0.08, 0.12)
	11kb promoters		0.08 (0.07, 0.1)	0.07 (0.05, 0.09)	0.08 (0.06, 0.09)
	TFBSs within 11kb promoters	CRMs	0.06 (0.04, 0.07)	0.04 (0.03, 0.06)	0.04 (0.03, 0.06)
		cistromes	0.07 (0.06, 0.09)	0.08 (0.06, 0.1)	0.09 (0.07, 0.11)
		cismotifs	0.07 (0.06, 0.09)	0.06 (0.05, 0.08)	0.07 (0.05, 0.08)
	Brain-specific colocalized regions	11kb promoters	0.09 (0.07, 0.11)	0.09 (0.07, 0.11)	0.11 (0.09, 0.13)
		genome	0.28 (0.25, 0.31)	0.26 (0.24, 0.29)	0.28 (0.26, 0.31)

For each noncoding variant set tested, power values for quantitative burden testing through logistic regression and specific to the variant count per child predictor are reported. Power was computed with a posthoc approach (for the observed ASD OR and at the current sample size) using three different simulation strategies (simr powerSim() function, “sample” custom function, and “random” custom function). Power was estimated over 1,000 simulations. A description of the simulation strategies can be found in the related SI Methods’ section. 95% confidence intervals for the power values are shown within parentheses.

**Dataset S1.** Sample demographics, family relationships, and whole-genome sequencing metrics.

**Dataset S2.** Detailed TADA results including qualifying variants, cohorts included, results, and results by variant class.

**Dataset S3.** Comparison table of TADA ASD risk gene identified at  $FDR < 0.1$ , Known ASD risk gene, and development disorder risk gene lists. A "1" indicates the inclusion of a gene within the gene list, while a "0" represents the absence of a gene in that list.

**Dataset S4.** List of AGRE ASD multiplex family samples overlapping with the MSSNG project cohort.

**Dataset S5.** Results from Poisson tests performed for variant rate comparison between AGRE multiplex families and ASD simplex family-based collections. Referring to Figures S6 and S9C.



## SI References

1. E. K. Ruzzo, *et al.*, Inherited and De novo Genetic Risk for Autism Impacts Shared Networks. *Cell* **178**, 850-866.e26 (2019).
2. X. Zhou, *et al.*, Integrating de novo and inherited variants in 42,607 autism cases identifies mutations in new moderate-risk genes. *Nat. Genet.* **54**, 1305–1319 (2022).
3. J. M. Fu, *et al.*, Rare coding variation provides insight into the genetic architecture and phenotypic context of autism. *Nat. Genet.* **54**, 1320–1331 (2022).
4. M. J. Maenner, *et al.*, Prevalence of Autism Spectrum Disorder Among Children Aged 8 Years - Autism and Developmental Disabilities Monitoring Network, 11 Sites, United States, 2016. *Morb. Mortal. Wkly. Rep. Surveill. Summ. Wash. DC 2002* **69**, 1–12 (2020).
5. E. Fombonne, Epidemiology of pervasive developmental disorders. *Pediatr. Res.* **65**, 591–598 (2009).
6. D. M. Werling, D. H. Geschwind, Sex differences in autism spectrum disorders. *Curr. Opin. Neurol.* **26**, 146–153 (2013).
7. W. M. Brandler, *et al.*, Paternally inherited cis-regulatory structural variants are associated with autism. *Science* **360**, 327–331 (2018).
8. S. Jacquemont, *et al.*, A higher mutational burden in females supports a “female protective model” in neurodevelopmental disorders. *Am. J. Hum. Genet.* **94**, 415–425 (2014).
9. Deciphering Developmental Disorders Study, Prevalence and architecture of de novo mutations in developmental disorders. *Nature* **542**, 433–438 (2017).
10. B. Trost, *et al.*, Genomic architecture of autism from comprehensive whole-genome sequence annotation. *Cell* **185**, 4409-4427.e18 (2022).
11. 1000 Genomes Project Consortium, *et al.*, A global reference for human genetic variation. *Nature* **526**, 68–74 (2015).
12. K. J. Karczewski, *et al.*, The mutational constraint spectrum quantified from variation in 141,456 humans. *Nature* **581**, 434–443 (2020).
13. M. Lek, *et al.*, Analysis of protein-coding genetic variation in 60,706 humans. *Nature* **536**, 285–291 (2016).
14. S. Purcell, *et al.*, PLINK: a tool set for whole-genome association and population-based linkage analyses. *Am. J. Hum. Genet.* **81**, 559–575 (2007).
15. G. Jun, *et al.*, Detecting and estimating contamination of human DNA samples in sequencing and array-based genotype data. *Am. J. Hum. Genet.* **91**, 839–848 (2012).
16. M. A. DePristo, *et al.*, A framework for variation discovery and genotyping using next-generation DNA sequencing data. *Nat. Genet.* **43**, 491–498 (2011).
17. G. A. Van der Auwera, *et al.*, From FastQ data to high confidence variant calls: the Genome Analysis Toolkit best practices pipeline. *Curr. Protoc. Bioinforma. Ed. Board Andreas Baxevanis AI* **11**, 11.10.1-11.10.33 (2013).

18. H. Li, *et al.*, The Sequence Alignment/Map format and SAMtools. *Bioinformatics* **25**, 2078–2079 (2009).
19. J. M. Zook, *et al.*, Integrating human sequence data sets provides a resource of benchmark SNP and indel genotype calls. *Nat. Biotechnol.* **32**, 246–251 (2014).
20. M. Gheorghe, *et al.*, A map of direct TF-DNA interactions in the human genome. *Nucleic Acids Res.* **47**, e21 (2019).
21. I. E. Vorontsov, *et al.*, Genome-wide map of human and mouse transcription factor binding sites aggregated from ChIP-Seq data. *BMC Res. Notes* **11**, 756 (2018).
22. D. Xu, C. Wang, K. Kiryluk, J. D. Buxbaum, I. Ionita-Laza, Co-localization between Sequence Constraint and Epigenomic Information Improves Interpretation of Whole-Genome Sequencing Data. *Am. J. Hum. Genet.* **106**, 513–524 (2020).
23. P. Green, C. J. MacLeod, SIMR: an R package for power analysis of generalized linear mixed models by simulation. *Methods Ecol. Evol.* **7**, 493–498 (2016).
24. D. M. Werling, *et al.*, An analytical framework for whole-genome sequence association studies and its implications for autism spectrum disorder. *Nat. Genet.* **50**, 727–736 (2018).
25. L. C. Francioli, *et al.*, Genome-wide patterns and properties of de novo mutations in humans. *Nat. Genet.* **47**, 822–826 (2015).
26. J. M. Goldmann, *et al.*, Parent-of-origin-specific signatures of de novo mutations. *Nat. Genet.* **48**, 935–939 (2016).
27. J. J. Michaelson, *et al.*, Whole-genome sequencing in autism identifies hot spots for de novo germline mutation. *Cell* **151**, 1431–1442 (2012).
28. S. Besenbacher, *et al.*, Multi-nucleotide de novo Mutations in Humans. *PLoS Genet.* **12**, e1006315 (2016).
29. D. F. Conrad, *et al.*, Variation in genome-wide mutation rates within and between human families. *Nat. Genet.* **43**, 712–714 (2011).
30. A. Kong, *et al.*, Rate of de novo mutations and the importance of father’s age to disease risk. *Nature* **488**, 471–475 (2012).
31. T. N. Turner, *et al.*, Genome Sequencing of Autism-Affected Families Reveals Disruption of Putative Noncoding Regulatory DNA. *Am. J. Hum. Genet.* **98**, 58–74 (2016).
32. R. K. Yuen, *et al.*, Whole genome sequencing resource identifies 18 new candidate genes for autism spectrum disorder. *Nat. Neurosci.* **20**, 602–611 (2017).
33. S. De Rubeis, *et al.*, Synaptic, transcriptional and chromatin genes disrupted in autism. *Nature* **515**, 209–215 (2014).
34. I. A. Adzhubei, *et al.*, A method and server for predicting damaging missense mutations. *Nat. Methods* **7**, 248–249 (2010).
35. I. Iossifov, *et al.*, The contribution of de novo coding mutations to autism spectrum disorder. *Nature* **515**, 216–221 (2014).

36. S. J. Sanders, *et al.*, Insights into Autism Spectrum Disorder Genomic Architecture and Biology from 71 Risk Loci. *Neuron* **87**, 1215–1233 (2015).
37. D. Pinto, *et al.*, Convergence of genes and cellular pathways dysregulated in autism spectrum disorders. *Am. J. Hum. Genet.* **94**, 677–694 (2014).
38. D. Polioudakis, *et al.*, A single cell transcriptomic atlas of human neocortical development during mid-gestation. *Neuron* **103**, 785-801.e8 (2019).
39. R. Satija, J. A. Farrell, D. Gennert, A. F. Schier, A. Regev, Spatial reconstruction of single-cell gene expression data. *Nat. Biotechnol.* **33**, 495–502 (2015).
40. N. G. Skene, S. G. N. Grant, Identification of Vulnerable Cell Types in Major Brain Disorders Using Single Cell Transcriptomes and Expression Weighted Cell Type Enrichment. *Front. Neurosci.* **10**, 16 (2016).
41. A. Dobin, *et al.*, STAR: ultrafast universal RNA-seq aligner. *Bioinforma. Oxf. Engl.* **29**, 15–21 (2013).
42. B. Li, C. N. Dewey, RSEM: accurate transcript quantification from RNA-Seq data with or without a reference genome. *BMC Bioinformatics* **12**, 323 (2011).
43. M. C. Oldham, P. Langfelder, S. Horvath, Network methods for describing sample relationships in genomic datasets: application to Huntington’s disease. *BMC Syst. Biol.* **6**, 63 (2012).
44. A. McKenna, *et al.*, The Genome Analysis Toolkit: a MapReduce framework for analyzing next-generation DNA sequencing data. *Genome Res.* **20**, 1297–1303 (2010).
45. J. T. Leek, W. E. Johnson, H. S. Parker, A. E. Jaffe, J. D. Storey, The sva package for removing batch effects and other unwanted variation in high-throughput experiments. *Bioinforma. Oxf. Engl.* **28**, 882–883 (2012).
46. W. S. Cleveland, S. J. Devlin, Locally Weighted Regression: An Approach to Regression Analysis by Local Fitting. *J. Am. Stat. Assoc.* **83**, 596–610 (1988).
47. H. Wickham, *ggplot2: Elegant Graphics for Data Analysis* (Springer-Verlag, 2009) <https://doi.org/10.1007/978-0-387-98141-3> (June 1, 2021).
48. M. Li, *et al.*, Integrative functional genomic analysis of human brain development and neuropsychiatric risks. *Science* **362** (2018).
49. Y. Liao, G. K. Smyth, W. Shi, featureCounts: an efficient general purpose program for assigning sequence reads to genomic features. *Bioinforma. Oxf. Engl.* **30**, 923–930 (2014).
50. P. Langfelder, S. Horvath, WGCNA: an R package for weighted correlation network analysis. *BMC Bioinformatics* **9**, 559 (2008).
51. G. Yu, L.-G. Wang, Y. Han, Q.-Y. He, clusterProfiler: an R package for comparing biological themes among gene clusters. *Omics J. Integr. Biol.* **16**, 284–287 (2012).
52. F. K. Satterstrom, *et al.*, Large-Scale Exome Sequencing Study Implicates Both Developmental and Functional Changes in the Neurobiology of Autism. *Cell* **180**, 568-584.e23 (2020).

53. M. J. Gandal, *et al.*, Shared molecular neuropathology across major psychiatric disorders parallels polygenic overlap. *Science* **359**, 693–697 (2018).
54. A. F. Pardiñas, *et al.*, Common schizophrenia alleles are enriched in mutation-intolerant genes and in regions under strong background selection. *Nat. Genet.* **50**, 381–389 (2018).
55. D. M. Ruderfer, *et al.*, Genomic Dissection of Bipolar Disorder and Schizophrenia, Including 28 Subphenotypes. *Cell* **173**, 1705-1715.e16 (2018).
56. A. Okbay, *et al.*, Genome-wide association study identifies 74 loci associated with educational attainment. *Nature* **533**, 539–542 (2016).
57. B. J. Vilhjálmsson, *et al.*, Modeling Linkage Disequilibrium Increases Accuracy of Polygenic Risk Scores. *Am. J. Hum. Genet.* **97**, 576–592 (2015).
58. D. J. Weiner, *et al.*, Polygenic transmission disequilibrium confirms that common and rare variation act additively to create risk for autism spectrum disorders. *Nat. Genet.* **49**, 978–985 (2017).
59. M. de Onis, WHO Motor Development Study: Windows of achievement for six gross motor development milestones. *Acta Paediatr.* **95**, 86–95 (2006).
60. J. N. Constantino, C. Gruber, *Social Responsiveness Scale, Second Edition (SRS-2)*. (Western Psychological Services, 2012).
61. K. Lyall, *et al.*, Parental Social Responsiveness and Risk of Autism Spectrum Disorder in Offspring. *JAMA Psychiatry* **71**, 936–942 (2014).
62. J. K. Lowe, D. M. Werling, J. N. Constantino, R. M. Cantor, D. H. Geschwind, Social responsiveness, an autism endophenotype: genomewide significant linkage to two regions on chromosome 8. *Am. J. Psychiatry* **172**, 266–275 (2015).